RSC Advances

REVIEW

View Article Online
View Journal | View Issue

Cite this: *RSC Adv.*, 2026, **16**, 29556

Research progress on two-dimensional phthalocyanine materials: from molecular design to exploration of multifunctional applications

Debing Long,[a] Xunyu Yang,[a] Zihao Cheng,[a] Cui Wang*[b] and Shan Peng*[a]

Two-dimensional (2D) phthalocyanine materials are periodic and ordered material systems formed by extending phthalocyanine or metal phthalocyanine molecules as structural units within a 2D plane through covalent or non-covalent interactions. As planar macrocyclic molecules with an 18π-electron conjugated system, phthalocyanine compounds provide an ideal molecular platform for constructing functional 2D materials due to their high structural stability, excellent physicochemical properties, and flexible molecular modifiability. This article systematically reviews the research progress of 2D phthalocyanine materials from molecular design to functional applications. Firstly, the discovery process, molecular structural characteristics, synthesis methods, and basic properties of phthalocyanine compounds as building blocks are introduced. Then, the structural basis, classification system, and top-down and bottom-up synthesis strategies of 2D phthalocyanine materials are elaborated. In terms of property research, the electronic structure and magnetic tuning mechanism of 2D phthalocyanine materials are discussed in detail, revealing the regulatory effects of central metal type, axial ligand modification, α-site substitution, and strain engineering on the material's band structure, magnetic ground state, and topological properties. The characteristic optical absorption (B-band and Q-band) of phthalocyanine compounds and their tuning strategies in the near-infrared region are systematically analyzed, and the optical application progress of 2D phthalocyanine materials in optoelectronic devices, photodynamic therapy, and other fields is summarized. In addition, the application exploration of these materials in catalytic conversion, gas detection and separation, clean energy storage, and other fields is reviewed, demonstrating their research value as multifunctional platforms. Finally, in response to the current challenges such as limited elemental systems, single network configurations, and insufficient optoelectronic performance, future research directions including expanding the main-group element system, innovating 2D network configurations, and achieving synergistic chemical modification and physical regulation are proposed. This review aims to provide a systematic theoretical reference for the rational design and functional application of 2D phthalocyanine materials.

Received 9th May 2026
Accepted 26th May 2026

DOI: 10.1039/d6ra03995b

rsc.li/rsc-advances

1. Introduction

The macroscopic physical properties and application potential of 2D materials fundamentally depend on the inherent characteristics of their constituent units and the assembly methods of these units within the 2D plane. Over the past two decades, 2D materials have emerged as a highly promising class of nanomaterials, encompassing graphene, transition metal dichalcogenides, hexagonal boron nitride, MXenes, layered double hydroxides, metal–organic frameworks, covalent organic frameworks, and many others.[1–5] Identifying molecular building blocks that possess both excellent intrinsic properties and high structural tunability is a core scientific issue in the design of novel functional 2D materials. Phthalocyanine (Pc) compounds, as a class of classic organic functional molecules, precisely meet this demand due to their unique molecular structure. Since their accidental discovery in the early 20th century, Pc compounds have undergone a century of development, evolving from their initial role as dyes and pigments into a star molecular system encompassing multifunctional applications in optics, electronics, magnetics, and catalysis.[1–4] A deep understanding of the structure and properties of Pc compounds is a necessary prerequisite and theoretical foundation for the rational design and construction of their 2D derivatives.

An individual Pc molecule possesses an 18π-electron conjugated system with a HOMO–LUMO gap of typically 1.5–2.0 eV, endowing it with intrinsic semiconducting properties. According to the Gouterman four-orbital model, the characteristic Q-band (600–700 nm) and B-band (300–400 nm)

[a]*School of Physics and Electronic-Information Engineering, Hubei Engineering University, Xiaogan, 432000, China. E-mail: pengshan@hbeu.edu.cn*
[b]*School of Chemistry and Chemical Engineering, University of South China, Hengyang 421001, China. E-mail: wangcui96@163.com*

correspond to $\pi \rightarrow \pi^*$ transitions. The frontier orbital levels and bandgap can be effectively tuned by selecting different central metals or peripheral substituents, providing a molecular basis for assembling Pc units into 2D materials with tailored macroscopic properties. The highly delocalized 18π-electron conjugated system and approximate D_{4h} planar tetragonal symmetry provide structural guarantees for their ordered stacking and efficient carrier transport within the 2D plane.[5,6] The central cavity of Pc can accommodate more than 70 metal ions, forming metal phthalocyanine (MPc) complexes with tunable magnetic, catalytic, and electronic properties.[7–9] Furthermore, various substituents can be introduced into the peripheral benzene rings (α- or β-positions) to achieve chemical modification of the molecule's solubility, stacking mode, and energy level structure,[10,11] while axial sites can coordinate with functional ligands to further expand the functional dimensions.[12,13]

Recent years have witnessed significant breakthroughs in phthalocyanine-based 2D materials and their applications. Theoretical studies have predicted a new class of 2D p-block main group phthalocyanine monolayers with exceptional carrier mobility exceeding 10^6 cm^2 V^{-1} s^{-1} and record power conversion efficiencies up to 26.28% in heterojunctions.[14] These findings open new avenues for flexible electronics and solar cell applications. In parallel, experimental advances have demonstrated precise control over stacking configurations in FePc covalent organic frameworks, where the eclipsed AA-stacked configuration exhibits a high-spin state of Fe that significantly enhances oxygen reduction reaction activity, achieving a half-wave potential of 0.856 V *vs.* RHE.[15] Metallophthalocyanine-based 2D nanomaterials have demonstrated remarkable performance in electrocatalytic energy conversion, including hydrogen evolution, oxygen reduction, and CO_2 reduction reactions.[16] Interfacial charge-transfer hybrids combining transition metal dichalcogenides (TMDs) with phthalocyanines have revealed strong ground-state and excited-state electronic coupling, with charge-separated state lifetimes on the order of hundreds of picoseconds, underscoring their potential in optoelectronic devices.[17]

The unique optical properties of Pcs, particularly their strong absorption in the Q-band region (600–700 nm) and tunable HOMO–LUMO gaps (typically 1.5–2.0 eV), make them ideal building blocks for optoelectronic devices and photocatalysts.[18,19] In the biomedical field, phthalocyanine-based photosensitizers continue to advance photodynamic therapy (PDT). Recent studies have demonstrated that metal-ion-induced H-type and J-type aggregation can significantly enhance singlet oxygen quantum yields, with ZnPc derivatives showing promise as PDT photosensitizers.[20] Nanoparticle-mediated delivery strategies have further improved the solubility, stability, and tumor-targeting capabilities of MPcs, addressing key clinical translation barriers.[21] Additionally, the modulation of Pc assembly morphology, through water-soluble non-aggregated forms, switchable aggregates, or stable aggregates, has emerged as a powerful strategy to optimize PDT outcomes.[22]

In the field of energy conversion, phthalocyanine-based metal–organic frameworks (MOFs) and covalent organic frameworks (COFs) have emerged as promising materials for photo- and electrochemical applications.[23] These hybrid materials integrate the exceptional electronic and catalytic properties of Pcs with the ordered frameworks of MOFs and COFs, offering enhanced charge transport and redox activity. Charge transport studies of silicon(IV) and zinc(II) phthalocyanines have revealed that silicon-based systems exhibit superior conductance with transmission peaks near the Fermi level, making them promising candidates for solar cell applications.[24] These recent advances across multiple disciplines underscore the growing importance of phthalocyanines as a versatile platform for functional 2D materials.

Therefore, understanding the structural chemistry and physical properties of Pc monomers and mastering their self-assembly rules and synthesis methodologies are essential for the development of functional 2D Pc materials. This review will begin with the discovery history, molecular structural characteristics, synthesis methods, and basic properties of Pc compounds, laying a solid foundation for subsequent in-depth exploration of the construction, performance tuning, and multifunctional applications of their 2D derivatives.

2. Phthalocyanine compounds

Pc compounds are the basic structural units for constructing 2D Pc materials. The discovery of these compounds can be traced back to 1907,[25] when Braun and Tehemiac of the London Gas Company accidently obtained a blue precipitate during the heating of *o*-cyanobenzamide and hexanol. However, due to the limitations of analytical techniques at that time, the two researchers did not identify or name the chemical structure of the blue substance; the compound was later confirmed to be Pc. In 1927, DeDiesbach and Wein of the University of Freiburg in Germany accidently obtained a blue compound with extremely high stability to acids, bases, and heat when attempting to prepare Pc by heating *o*-dibromobenzene and cuprous cyanide in pyridine.[26] In 1928, a dye factory in Scotland accidently produced a blue precipitate (later confirmed as a Pc compound) during the production of phthalimide (prepared from phthalic anhydride) due to the rupture of a glass pipeline, which allowed the reaction materials to come into contact with the steel shell. Given the bright color of this by-product and its excellent stability to air, acids, and bases, researchers subsequently isolated and developed it into a new type of dye. It was not until 1934 that Linstead and others at Imperial College London conducted a systematic study of this type of colored compounds and named them "Pc".[27] The following year, Robertson successfully resolved the crystal structure of Pc molecules using X-ray diffraction technology (Fig. 1a and b).[28] In addition, in 2012, Kobayashi *et al.* first reported expanded Pc molecules with bimetallic centers (Fig. 1c and d), which were synthesized by heating a mixture of phthalic anhydride or phthalimide and excess urea at 210−250 °C in the presence of molybdenum or tungsten salts.[29] The discovery of expanded Pc molecules further enriched the Pc family of materials.

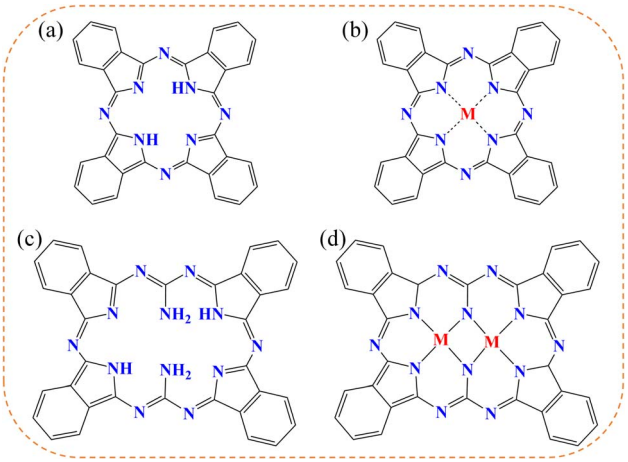

Fig. 1 Chemical structures of Pc and its derivatives. (a) Metal-free Pc and (b) metal Pc. (c) Expanded Pc and (d) bimetallic expanded Pc.

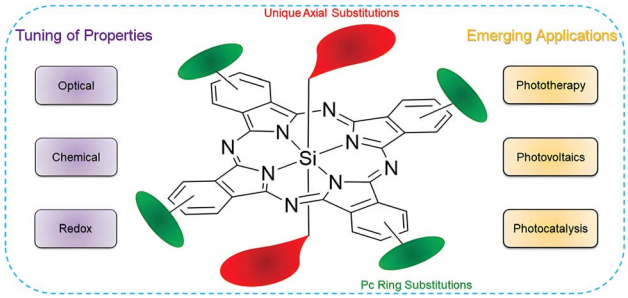

Fig. 2 (a) Schematic diagram of property regulation and different applications of Pc compounds based on chemical modification. Reproduced with permission from ref. 31. Copyright [2021] [Royal Society of Chemistry].

2.1. Structural foundations of phthalocyanine compounds

From the molecular structure (Fig. 1a), Pc is formed by the bridging of four isoindole units through imino (–N=) bonds, creating a planar sixteen-membered ring that constitutes an 18π-electron conjugated system with alternating nitrogen and carbon atoms (conforming to the Hückel's $4n + 2$ rule, $n = 4$). The highly delocalized electron cloud distribution maintains low distortion in the four benzene rings within the molecule, and all C–N bond lengths tend to be equal. This highly symmetric conjugated structure endows it with significant aromaticity and chemical stability. MPcs is a class of functional complexes formed by the coordination of Pc macrocyclic ligands with metal ions. The choice of central metal significantly affects its structure and physicochemical properties. Transition metals usually form single-layer Pc complexes, while metals with higher coordination numbers (such as rare earth elements) tend to form sandwich-like structures. Currently, over 70 metals are known to coordinate within the Pc cavity, and their ionic radii, charges, and coordination configurations directly regulate the electronic properties of the complexes. Pc molecules are highly modifiable: substituents can be introduced at α/β positions (forming unsubstituted, monosubstituted, or fully substituted derivatives),[30] while axial sites are functionalized through metal coordination.[31] The modification of central metal and peripheral substituent groups collectively alters the electron cloud distribution of the entire conjugated system, thereby affecting its photophysical, photochemical, and electrochemical behaviors (Fig. 2).

Pc compounds exhibit excellent optical, electrical, and magnetic properties due to their 2D macrocyclic conjugated structure and delocalized π-electron system. Initially used primarily as dyes and pigments, they have now expanded into high-tech fields such as optical limiting materials,[32–34] nonlinear optical materials,[35,36] gas sensing materials,[37–39] liquid crystal display materials,[40,41] catalysts,[42–44] molecular semiconductor materials,[45,46] molecular magnets,[47,48] molecular electronic devices,[49,50] and photodynamic cancer therapy.[51,52]

After more than a century of development, the Pc system has expanded from hollow structures to over 70 metal complexes, evolving from single-layer derivatives to sandwich structures, dendritic derivatives, subphthalocyanines, polymeric Pcs, and other variants. Additionally, water-soluble and asymmetric novel derivatives have been developed. With a long research history and sustained vitality, Pcs have become a research hotspot in modern materials science due to their multifunctional properties, holding broad application prospects in fields such as photoelectric conversion, catalytic synthesis, and nanodevices.

2.2. Synthesis methods of phthalocyanine compounds

The raw materials for the synthesis of Pc primarily include *o*-aminobenzamide, phthalonitrile, and 1,3-diaminoisoindole. When *o*-aminobenzamide is used as the raw material, it is reacted at 230 °C in the presence of metals (such as Mg and Sb) or their oxides, and then treated with concentrated sulfuric acid, achieving a yield of up to 40%.[53] The phthalonitrile route can directly yield Pc with a high yield (90%) by heating ammonia gas in *N*,*N*-dimethylethanolamine,[54] or through a sodium alkoxide/acid treatment pathway.[55] 1,3-Diaminoisoindole (prepared by hydrogenation of phthalonitrile) can be refluxed in *N*,*N*-dimethylethanolamine to obtain Pc with a yield of 85%.[56]

The synthesis of metal Pcs primarily employs a template reaction method, with core raw materials including phthalic anhydride-urea, phthalonitrile, and metal salts. The specific pathways are as follows: (1) the phthalic anhydride-urea method is commonly used for the industrial production of ZnPc, *etc.*;[57,58] (2) the target complex is obtained by replacing LiPc with metal halides; (3) synthesis of phthalonitrile and metal salts under reflux conditions in *N*,*N*-dimethylethanolamine, high-boiling alcohol (catalyzed by DBU), or 1-chlorobenzene, where the alcohol solvent system yields fewer by-products and higher yields;[59] (4) solid-phase synthesis using phthalic anhydride and urea. Hydrothermal synthesis, as an emerging approach, utilizes phthalonitrile, metal powder (such as copper), and ammonium molybdate as raw materials to prepare nanostructured Pcs under hydrothermal conditions at 150–180 °C for 5 days.[60] Its advantages include using water as a green solvent to

reduce pollution, low cost, and precise control of crystal growth by adjusting temperature, pressure, and pH parameters, yielding high-purity products with good crystallinity and controllable morphology (such as nitro/iodo-substituted Pcs) in a closed system, thus providing an efficient pathway for the preparation of functional materials.[61–63]

The synthesis system of Pc compounds has evolved into a multi-path reaction mode using *o*-aminobenzamide, phthalonitrile, and their derivatives as raw materials. By combining strategies such as metal-template cyclization, solid-phase condensation, and hydrothermal synthesis, efficient and precise construction from free Pc to metal Pc has been achieved. The metal-template reaction enables directional regulation of the ligand assembly process, while hydrothermal synthesis relies on high-temperature and high-pressure aqueous environments to achieve functional design of crystal morphology and substituents. Together, these methods provide a methodological foundation for molecular structure customization, metal center selection, and nanostructure control of 2D Pc materials. The breakthroughs in substituent modification, coordination microenvironment optimization, and spatial dimensional control achieved by these synthesis techniques strongly support subsequent research on the controllable preparation and performance optimization of 2D Pc materials.

3. 2D phthalocyanine materials

As an important branch of modern materials science, 2D materials offer new insights into the design of optoelectronic functional materials due to their unique quantum confinement effects and anisotropic properties. In this context, Pc compounds, as 18π-electron conjugated macrocyclic systems, have emerged as highly promising members of the 2D material family, thanks to their flexibility in central metal coordination, peripheral group modification, and axial ligand design. 2D Pc materials are periodic and ordered material systems formed by extending Pc or metal Pc molecules as structural units within a 2D plane through covalent or non-covalent interactions. Their structural foundation stems from the 18π-electron conjugated macrocyclic characteristics and fourfold axial symmetry (D_{4h} point group) of the Pc unit, achieving long-range ordered assembly within the plane through connection modes such as intermolecular benzene ring sharing (vertex connection or edge sharing), metal coordination, or π–π stacking. These materials follow mathematical tiling patterns (such as Archimedean tiling) to form an extended network structure with regular pores. The essential characteristic of 2D Pc materials lies in breaking through the discrete nature of monomer molecules, constructing layered materials with atomic-level thickness, continuous π-conjugated backbones, and tunable electronic structure. Their physicochemical properties are synergistically determined by the valence state of the central metal ion, peripheral substituents, and topological configuration (such as square or Kagome lattices).

The classification of 2D Pc materials can be based on factors such as central element and substituent type. A systematic classification with representative examples is as follows: The

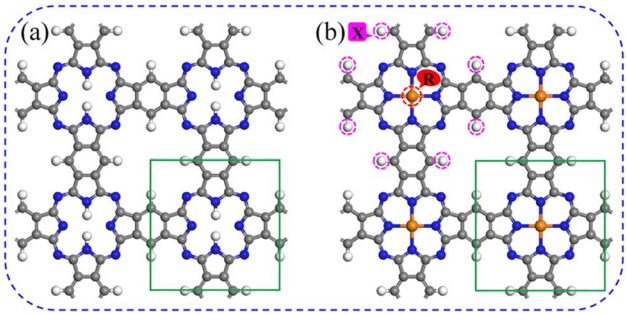

Fig. 3 2D (a) H_2Pc and (b) MPc monolayers, where (b) exhibits α-site substitution and axial ligand coordination configurations.

central elements of 2D Pc materials can be divided into three categories (Fig. 3): (1) metal-free Pc 2D materials (H_2Pc): their centers consist of two hydrogen atoms, possessing an 18-π electron aromatic structure and belonging to planar macrocyclic conjugated molecules. These materials do not introduce metal ions, thus retaining the original electronic structural characteristics of Pc.[64] (2) Main-group metal Pc materials: the central hydrogen atoms are replaced by main-group metal ions (such as Zn and Al) to form a metal-nitrogen coordination structure. For example, ZnPc coordinates with the nitrogen atoms of the Pc ring through the central Zn ion, significantly affecting the molecular electron cloud distribution and photophysical properties.[65] (3) Transition metal Pc materials: the central hydrogen atoms are replaced by transition metal ions (such as Cu, Co, Ni, and Fe). The choice of central metal directly affects the crystal structure, catalytic activity, and spectroscopic properties of the material. For instance, CuPc is widely used in optoelectronic materials,[66] while CoPc exhibits high catalytic activity in oxygen reduction reactions.[67]

3.1. Synthesis strategies and microscopic morphological characterization of 2D phthalocyanine materials

The synthesis of 2D Pc materials primarily follows two strategies: bottom-up and top-down. The bottom-up strategy involves the direct synthesis of 2D structures from molecular building blocks. Surface synthesis is a significant representative of this approach, typically conducted in ultra-high vacuum environments. Functional precursor molecules, such as tetracyanobenzene and metal atoms, are deposited onto specific single-crystal substrates (*e.g.*, Au(111), Ag(111), insulating modified substrates (*e.g.*, NaCl/Ag(100)), or graphene). Through stepwise regulation of substrate temperature and intermolecular forces (such as metal coordination bonds, hydrogen bonds, or high-temperature-induced covalent bonds), a gradual transformation from metal–organic coordination networks to Pc monomers is achieved *in situ* on the substrate surface, ultimately forming a long-range ordered monolayer of 2D Pc structures[68] (as shown in Fig. 4, experimentally prepared 2D FePc,[69] CuPc,[70] and MnPc monolayers[71]). Solvothermal synthesis constructs 2D Pc frameworks through liquid-phase reactions: MOF-based Pc systems are formed through metal coordination in aqueous solutions (*e.g.*, NiPc-NiO_4 prepared at

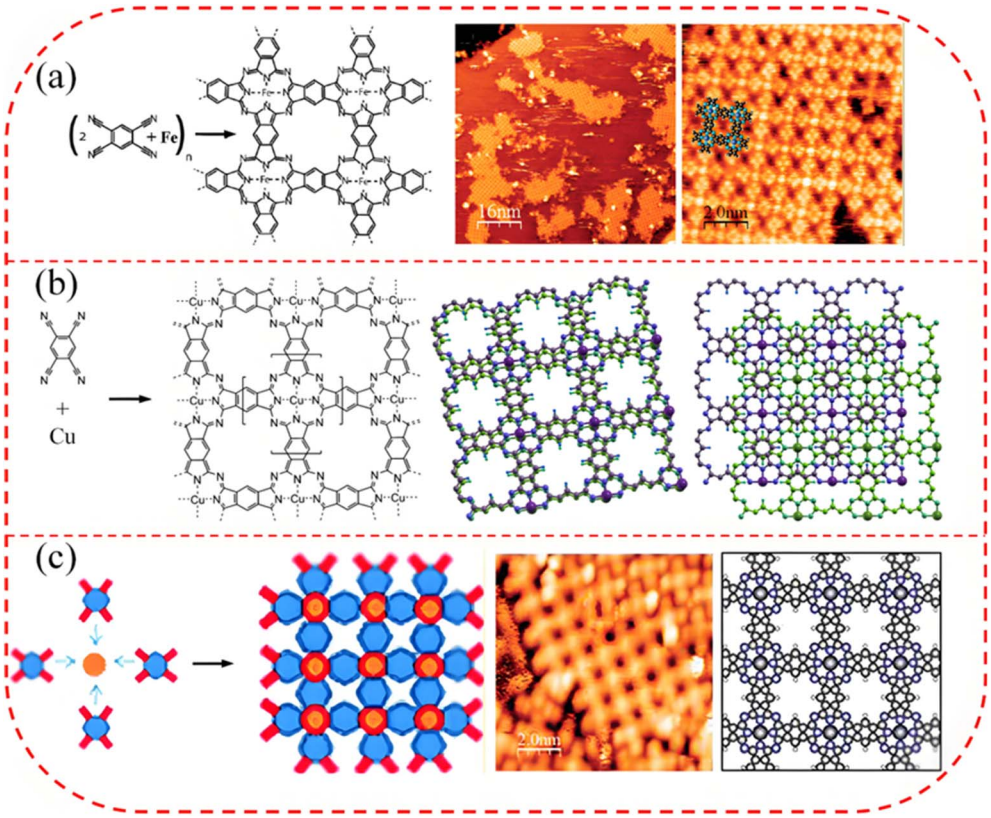

Fig. 4 The synthesis route and structural schematic diagram of 2D (a) FePc, (b) CuPc, and (c) MnPc monolayers. Reproduced with permission from ref. 69–71. Copyright [2011] [American Chemical Society], [2013] [Elsevier, Ltd], [2014] [Royal Society of Chemistry].

85 °C), while COF-based Pc systems are generated through covalent condensation in organic solvents (*e.g.*, CoPc-PI-COF synthesized at 120 °C). This method allows precise control of the crystal structure but requires optimization of solvents and bonding mechanisms based on the type of material.[72,73] Surface-mediated synthesis is carried out in ambient organic solvents (such as quinoline) through microwave radiation-driven self-assembly of precursor molecules (metal salts and organic ligands) to form Pc nanosheets. This method eliminates the need for interfacial assistance and produces polycrystalline structures, making it suitable for the large-scale preparation of electrocatalytic materials.[74]

The top-down strategy involves mechanical exfoliation and liquid-phase exfoliation to obtain 2D materials. The mechanical exfoliation method, centered around ball milling technology, utilizes interlayer agents and shear forces to disrupt interlayer interactions, achieving the thinning of Pc crystals (with the thinnest obtained being approximately 7 nm). This method is simple to operate and retains the crystal structure, but the product size is uneven, monolayers are difficult to obtain, and the efficiency of large-scale production is limited (yield < 50%).[75] The liquid-phase exfoliation method, with solvent ultrasonication as the core technology, disperses Pc bulk materials (such as $Fe_{0.5}Co_{0.5}$Pc-CP) in ethanol and, after ultrasonication treatment (300 W, 8 h), yields nanosheets with a thickness of approximately 1.05 nm (yield 51%). This method offers high yield and good dispersibility, but the product size distribution is wide (100 nm to 2 μm), crystallinity is lost (transformed into an amorphous phase), and no subsequent size separation is performed.[76]

Overall, the bottom-up approach (especially the surface synthesis method) exhibits significant advantages in preparing 2D Pc with precise atomic-level structure and long-range order, making it suitable for fundamental physical property research in ultra-high vacuum environments. Conversely, the top-down approach (particularly the liquid-phase exfoliation method) holds greater potential for large-scale production and solution processing applications (such as the macroscale preparation of electrocatalytic materials) due to its high production efficiency (yield > 50%) and solution dispersibility. The choice of method requires careful consideration of the target material's crystal quality, structural homogeneity requirements, application scenarios, and equipment cost constraints.

The morphological characterization of 2D phthalocyanine materials *via* scanning electron microscopy (SEM) and transmission electron microscopy (TEM) has provided critical insights into their nanostructures, layer stacking, and defect distributions. These microscopic techniques are essential for verifying the successful synthesis of ultrathin 2D morphologies and understanding structure–property relationships.

Liquid-phase exfoliation of bulk Pc crystals typically yields nanosheets with lateral dimensions ranging from hundreds of

nanometers to several micrometers. Liu *et al.* employed TEM to characterize $Fe_{0.5}Co_{0.5}$Pc-CP nanosheets exfoliated *via* ultrasonication in ethanol, revealing amorphous structures with thicknesses of approximately 1.05 nm and lateral sizes of 100 nm to 2 μm.[76] Selected area electron diffraction (SAED) patterns confirmed the loss of long-range crystallinity after exfoliation, which is consistent with the amorphous nature of the resulting nanosheets. Similarly, Wang *et al.* used TEM and atomic force microscopy (AFM) to characterize mechanically exfoliated Pc-based MOF nanosheets, showing that ball-milling-assisted exfoliation produced crystalline nanosheets with thicknesses around 7 nm, though monolayers remained difficult to obtain.[75] Bottom-up surface synthesis under ultra-high vacuum enables the fabrication of atomically precise 2D Pc monolayers with long-range order. Abel *et al.* used scanning tunneling microscopy (STM) and low-energy electron diffraction (LEED) to characterize a single-layer polymeric FePc sheet on Au(111) and thin NaCl/Ag(100) insulating films, demonstrating a well-ordered square lattice structure with lattice constants consistent with DFT calculations.[69] Sedlovets *et al.* employed TEM and AFM to study Cu polyphthalocyanine films synthesized *via* CVD, revealing continuous monolayer films with a thickness of approximately 0.7–1.0 nm and a polycrystalline structure composed of nano-grains.[70] Koudia and Abel used STM to monitor the stepwise on-surface synthesis of MnPc polymers, directly visualizing the transition from monomeric MnPc molecules to covalently linked 2D networks on Au(111) substrates.[71] For MOF-based and COF-based 2D Pc materials, TEM has been extensively used to confirm their layered morphologies. Yi *et al.* synthesized conductive NiPc-NiO_4 MOF nanosheets *via* a solvothermal method at 85 °C, and TEM images revealed ultrathin sheet-like morphologies with lateral dimensions of several hundred nanometers and thicknesses of 2–3 nm as determined by AFM.[72] High-resolution TEM (HRTEM) showed the presence of ordered micropores consistent with the simulated crystal structure. Lu *et al.* reported dioxin-linked CoPc-PI-COF nanosheets synthesized at 120 °C, and TEM characterization confirmed a 2D layered morphology with high crystallinity and a pore size of approximately 1.8 nm.[73] The HRTEM images clearly resolved the hexagonal lattice fringes, demonstrating the well-ordered porous network. Wang *et al.* developed a microwave-assisted method for the rapid synthesis of metallophthalocyanine nanosheets in ambient organic solvents such as quinoline.[74] TEM and SEM characterization revealed polycrystalline nanosheets with lateral sizes of 1–5 μm and thicknesses of 5–10 nm. The polycrystalline nature was confirmed by the presence of grain boundaries in HRTEM images and ring-like SAED patterns, which is advantageous for electrocatalytic applications due to the abundance of edge active sites.

Across these studies, several consistent observations emerge: (1) top-down exfoliation methods (mechanical, liquid-phase) yield nanosheets with preserved or partially preserved crystalline order, but often with limited control over lateral size and thickness uniformity; (2) bottom-up surface synthesis produces atomically precise 2D Pc monolayers with long-range order, but typically requires ultra-high vacuum conditions and conductive substrates, limiting scalability; (3) solution-based bottom-up methods (solvothermal, microwave) offer scalable routes to 2D Pc frameworks but often produce polycrystalline or amorphous nanosheets; (4) TEM and AFM are indispensable for verifying the 2D morphology, measuring layer thickness, and assessing crystallinity, while STM provides atomic-scale resolution of surface-adsorbed monolayers.

3.2. Basic properties of 2D phthalocyanine materials

2D Pc materials constitute a functional system that combines molecular conjugation characteristics with 2D nanostructure features. Their unique electronic structures (such as tunable bandgap characteristics) and optical properties (strong Q-band absorption) exhibit research value in fields such as optoelectronic devices and catalytic conversion. Based on these characteristics, researchers both domestically and internationally have conducted in-depth studies on these materials in recent years, aiming to explore their properties and expand their application scope. Meanwhile, this field also presents some new development trends. The electronic and optical properties of 2D Pc materials are crucial for their excellent performance. In terms of electronic properties, they exhibit certain carrier mobility and unique bandgap structures. For example, metal Pc frameworks based on polyarylene ether exhibit p-type semiconductor characteristics with high intrinsic mobility (19.4 $cm^2 V^{-1} s^{-1}$), and their conductivity is significantly improved after iodine doping.[77] In terms of optical properties, they exhibit strong absorption in the ultraviolet-visible light region, and their photophysical properties can be tuned by altering the metal center or peripheral substituents. These properties make 2D Pc materials promising for the preparation of high-tech products such as solar cells and optoelectronic devices. For example, transition metal Pcs can be used to prepare solar photovoltaic materials and spintronic devices.[78] In terms of future development trends, with the continuous deepening of research, researchers are focusing on optimizing their properties and expanding their functions, aiming to further broaden their application fields. It should be noted that research development in this field is uneven, with significant differences in reports on different properties, performances, and application directions. Among them, the magnetic and spintronic properties of 2D Pc materials are currently the most intensively researched directions, while there are relatively few reports on main-group Pcs, semiconductors, and their optoelectronic properties. In terms of future development trends, deepening research in existing advantageous directions and exploring weak links will jointly promote the comprehensive development of this field.

3.2.1. Electronic structure and magnetism of 2D phthalocyanine materials. In recent years, the electronic structure and magnetic properties tuning of 2D Pc materials have become a research hotspot both domestically and internationally. The focus is primarily on unveiling their unique magnetic coupling mechanisms and tunable electronic characteristics, laying the groundwork for novel spintronic devices. First, let us delve into the intrinsic semiconductor properties and non-magnetic

behavior of the 2D metal-free Pc (*i.e.*, H_2Pc) material system. Density functional theory (DFT) calculations reveal that H_2Pc material exhibit a direct bandgap (approximately 0.21–0.29 eV) in their equilibrium state.[79–81] The electronic states near the Fermi level are primarily contributed by the ligand p-orbitals, manifesting as a non-magnetic ground state (Fig. 5a and b).[81] External strain can significantly modulate its electronic behavior: biaxial tensile strain (such as 14.7%) flattens the energy bands by weakening the π-electron hopping integral, leading to an increased bandgap of 0.79 eV and an elevated effective mass of carriers. This material possesses excellent mechanical deformability, endowed by its low Young's modulus (73.41 J m^{-2}) and high Poisson's ratio (0.43).[79]

The electronic structure and magnetic properties of 2D Pc materials can be further precisely tuned through substituent modification. Substituent modification can be divided into α-position substitution and central metal axial substitution based on their positions. These two types of substitutions achieve performance tuning through ligand engineering and metal coordination, respectively. α-Position substitution involves functional group modification (such as halogen atoms) at non-peripheral sites of the isoindole ring. Its core mechanism lies in

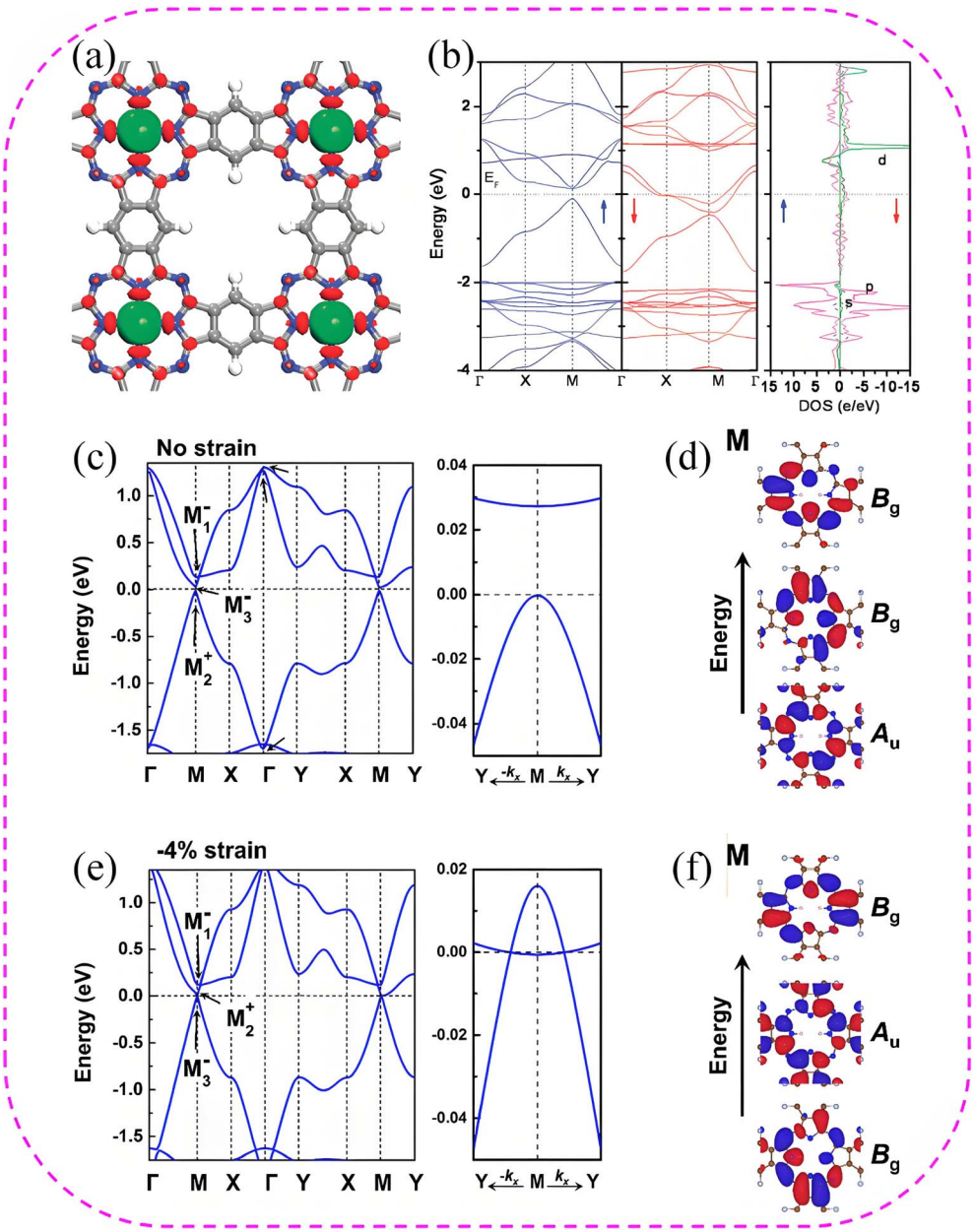

Fig. 5 (a) Geometric structure and (b) band structure and corresponding PDOS of 2D H_2Pc monolayer. Reproduced with permission from ref. 81. Copyright [2011] [American Chemical Society]. DFT-calculated band structures of the F-Pc COF (c) in the absence of strain and (e) under 4% compressive strain. The related wave functions at the M point are represented in (d) and (f), respectively. Reproduced with permission from ref. 80. Copyright [2022] [American Chemical Society].

regulating the local electronic structure of the ligand through the electronegativity of the substituent. For example, a highly electronegative substituent (−F) significantly reduces the local potential at edge sites, narrowing the energy level difference (ΔE) with the corner metal Pc unit, thereby decreasing the bandgap of the material (*e.g.*, H → F substitution in ZnPc-MOF reduces the bandgap from 0.291 to 0.111 eV).[82] α-Position halogen substitution can further expand the tuning dimension. After substitution with F, Cl, or Br, the strong electronegativity of the halogen induces a downward shift in the ligand energy levels and orbital hybridization, significantly reducing the bandgap of H-Pc to 0.027 eV (F-Pc), 0.077 eV (Cl-Pc), and 0.038 eV (Br-Pc) (at the PBE level), with F-Pc exhibiting the smallest bandgap, approaching a half-metallic state. It is worth noting that halogen substitution does not alter the non-magnetic nature of the material, but F-Pc can trigger Au-Bg band inversion under 4% biaxial compressive strain, achieving a phase transition from an insulator to a topological Dirac half-metal, as shown in Fig. 5c–f.[80] In summary, metal-free Pc materials achieve continuous tuning of their electronic structure from wide-bandgap semiconductors to topological quantum states through the synergistic effect of intrinsic design (halogen substitution) and external field tuning (strain engineering), providing a multi-dimensional design strategy for these materials.

Compared to the non-magnetic semiconductor characteristics of 2D metal-free Pc materials, the introduction of transition metal atoms significantly modulates their electronic structure and magnetic properties. Recent literature reports have primarily focused on transition metal systems within 2D Pc materials, particularly emphasizing the regulation of their magnetic behavior and potential applications in spintronics. Theoretical studies on the electronic structure and magnetism of 2D transition metal Pcs reveal that the valence state, orbital hybridization strength, and ligand environment of the central metal atom collectively determine the magnetic ground state and electronic properties of the material. Specifically, among the 3d series, only MnPc exhibits ferromagnetic half-metallic behavior (with a metallic spin-down channel), and its ferromagnetic coupling originates from the hybridization of d_{xz}/d_{yz} orbitals with ligand p orbitals. Monte Carlo simulations predict a Curie temperature (T_C) of approximately 150 K for MnPc. Meanwhile, CrPc, FePc, CoPc, and CuPc are antiferromagnetic, while NiPc and ZnPc are non-magnetic.[81] In the 4d/5d series, RuPc and RePc have been confirmed as ferromagnetic half-metals, with RuPc exhibiting a significantly higher magnetic exchange energy ($E_{ex} = 153.5$ meV per atom) compared to other systems. Mo-TCNB demonstrates unique properties as a ferromagnetic insulator ($E_{ex} = 71.8$ meV per atom).[83] Notably, the ligand environment significantly affects electronic correlation effects: linear response calculations indicate that the multi-site Hubbard U value, including the isoindole nitrogen atom (N_{iso}), is approximately 1 eV higher than that obtained from single-site calculations. This correction is crucial for accurately describing the electronic structure of chemisorption systems.[84] The aforementioned studies not only establish a classification framework for the magnetic order of MPc materials but also provide a theoretical basis for designing spintronic devices based on ferromagnetic half-metallic states, such as MnPc and RuPc.

Furthermore, axial substitution (R) of transition metals can directly reconstruct the metal center microenvironment through vertical coordination with non-metal atoms (such as Cl and F). For example, single-atom substitution increases the oxidation state of the metal from +2 to +3 (such as $Fe^{2+} \rightarrow Fe^{3+}$), and the crystal field weakens from planar tetragonal to tetragonal pyramidal, leading to a significant enhancement of the magnetic moment (such as the magnetic moment of FePc increases from 2 to 5 μ_B). Dual-atom substitution further induces p-type doping of the Pc skeleton and changes the magnetic coupling properties, with the MnPc system exhibiting unique reversible switching of magnetic order (unsubstituted FM → single Cl-substituted AFM → double Cl-substituted FM).[85] The strong binding energy (such as 4.01 eV for F-FePc) and thermal stability (>400 K) of axial substitution lay the foundation for the environmental adaptability of magnetic devices.[86]

Chemical modification of 2D Pc materials can also significantly regulate their electronic and magnetic properties. The introduction of axial ligands (such as non-metal atoms or chlorine) induces d-π orbital hybridization reconstruction by altering the coordination geometry and oxidation state of the central metal (such as the formation of high-spin Fe^{3+} state), achieving quantitative adjustment of magnetic moment (the adjustable range of magnetic moment in the FePc system is up to 0–5 μ_B) and magnetic order transition (such as antiferromagnetic/ferromagnetic transition in MnPc). Meanwhile, coordination bonding leads to band rearrangement, manifested as bandgap changes or Dirac cone evolution.[85,86] α-Halogen substitution (such as benzene ring H → F/Cl) significantly narrows the Dirac cone and bandgap (the bandgap of ZnPc-MOF decreases from 0.291 to 0.111 eV) by reducing the local potential energy at the edge-center sites. This effect, in conjunction with physical strain, can further induce topological non-trivial states (such as topological insulator phase transition in a Lieb lattice).[82] The aforementioned chemical modification strategies provide new avenues for material design of multifunctional quantum devices by precisely regulating electron filling, orbital coupling, and band topological properties. Having established the tunability of electronic structure and magnetism through chemical modification and external fields, we next examine the optical properties of 2D Pc materials.

3.2.2. Optical properties of 2D phthalocyanine materials. Building on the preceding discussion of electronic structure and magnetic properties, we now turn to the optical properties of 2D Pc materials. Given that systematic optical studies on 2D Pc materials remain relatively scarce compared to their magnetic counterparts, it is instructive to first establish the fundamental optical characteristics of Pc compounds at the molecular level. Accordingly, this section begins with an overview of the basic photophysical properties of Pc molecules, including their characteristic Q-band and B-band absorptions, before extending the discussion to the emerging optical behaviors and applications of their 2D derivatives. Pc molecules are 18π-electron planar macrocyclic conjugated systems formed

by four isoindole units connected *via* nitrogen bridges. Their highly delocalized π-electron system endows them with unique photophysical properties. Their UV-visible absorption spectra exhibit two characteristic absorption bands: the B band (Soret band) located in the near-UV region (300–400 nm) and the Q band distributed in the visible to near-infrared region (600–700 nm). According to the Gouterman four-orbital model, the Q band originates from the π → π* transition from the highest occupied molecular orbital (HOMO, a_{1u}) to the lowest unoccupied molecular orbital (LUMO, e_g), while the B band is generated by the π → π* transition from the low-energy occupied orbital (a_{2u}) to the e_g orbital.[87]

As shown in Fig. 6a and b, for metal-free Pc (H_2Pc), its lower D_{2h} symmetry leads to the lifting of e_g orbital degeneracy (splitting into e_{gx} and e_{gy}), resulting in the splitting of the Q band into two polarization components (around 660 and 700 nm), while the B band exhibits a single peak near 350 nm.[88] This bimodal absorption feature, caused by the non-degeneracy of molecular orbitals, can serve as a criterion for the formation of Pc ring cyclization. Additionally, the position of the substituent (α or β position) significantly affects its electronic structure. For example, electron-donating substituents can induce a red shift of the Q band by reducing the HOMO–LUMO energy gap. In metal Pcs, the coordination of central metal ions usually enhances the molecular symmetry to D_{4h}, maintaining the degeneracy of e_g orbitals, thus resulting in a single strong absorption peak of the Q band (around 670 nm). Metal ions not only enhance the rigidity of the ring through coordination but may also induce metal–ligand charge transfer, leading to a red shift of the B band to 320–400 nm. The participation of d orbitals from specific metals (such as Pb and Ti) can further induce charge transfer transitions, significantly broadening the near-infrared absorption range. The electronic effect of central metals can also modulate the position of the Q band; for example, metal ions such as Pb^{2+} and Ti^{4+} can promote a red shift of the Q band by reducing the HOMO–LUMO energy gap. Such tunable spectral characteristics endow Pc compounds with potential applications in fields such as optical limiting and

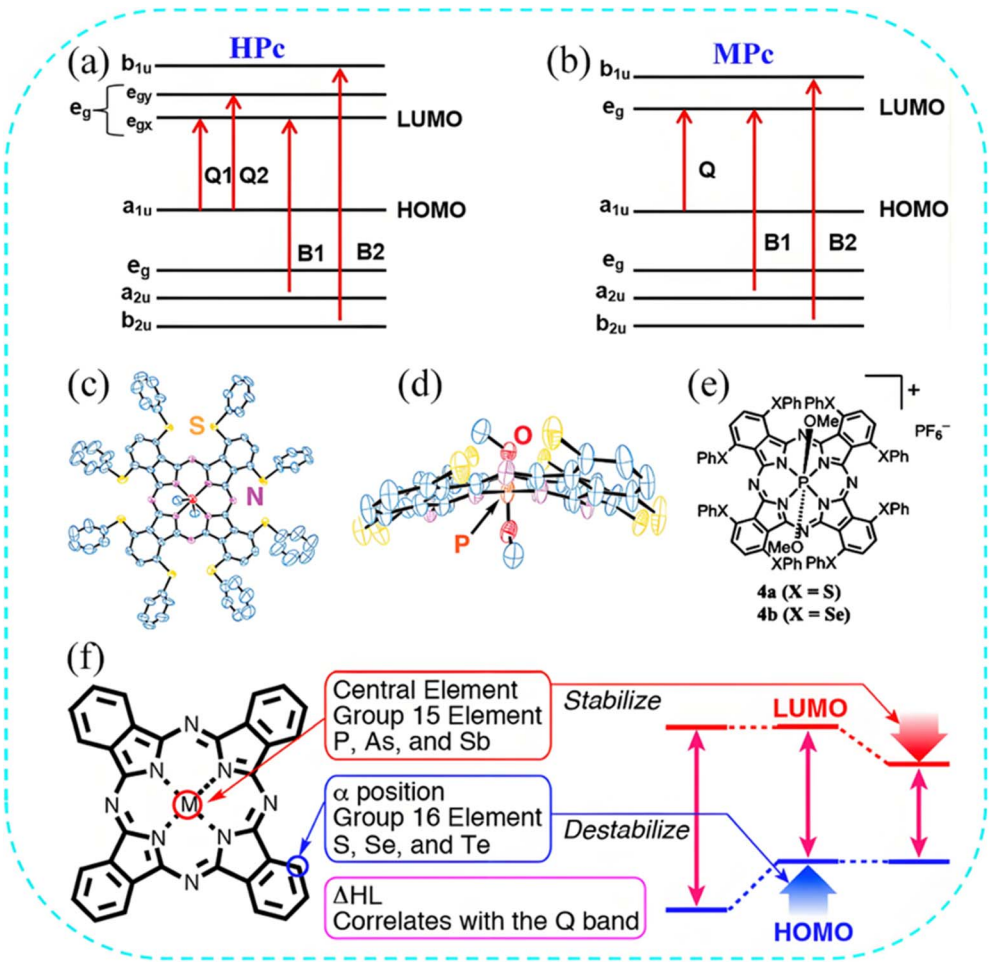

Fig. 6 Goutermans four-orbital model showing electron transitions and the origin of Q and B bands for (a) H_2Pc and (b) MPc. Reproduced with permission from ref. 87. Copyright [2020] [Elsevier, Ltd]. Thermal ellipsoid (50%) diagrams of the molecular structure of $[(PhS)_8PcP(OMe)_2][PF_6]$: (c) top view, (d) side view (peripheral substituents omitted), (e) chemical structure formula. Reproduced with permission from ref. 90. Copyright [2011] [American Chemical Society]. (f) Molecular design of NIR phthalocyanines. Reproduced with permission from ref. 91. Copyright [2014] [American Chemical Society].

photocatalysis. The spectral differences between metal-free Pc and metal Pc profoundly reveal the intrinsic correlation between molecular symmetry, orbital degeneracy, and electronic structure, providing important theoretical support for the rational design of functionalized Pc.[89]

To precisely tune the optical properties of Pc to meet the spectral characteristics required for specific applications, researchers have developed a synergistic strategy involving main-group elements, successfully designing a highly stable system with a main absorption band exceeding 1000 nm. Specifically, by introducing S or Se substituents at the α-position and combining them with central P(v) ions to form complexes (such as $[PcP(OMe)_2][PF_6]$, Fig. 6c–e), the Q-band absorption can be significantly red-shifted to 1018 and 1033 nm. This red-shifting effect originates from the significant stabilization of the LUMO energy level due to the strong electron-withdrawing effect of P(v), as well as the enhancement of the HOMO energy level by the electron-donating properties of the peripheral S/Se substituents, both of which collaboratively narrow the HOMO–LUMO energy gap. X-ray crystallography confirms that the introduction of P(v) leads to the wrinkling and deformation of the Pc ring ($\Delta r = 0.472$ Å), further promoting the absorption red shift. Both electrochemical and theoretical computational analyses support that the Q-band shift is primarily attributed to the stabilization of the LUMO and the partial destabilization of the HOMO, and such Pcs are stable in air for long periods.[90] This strategy has been further systematically extended to the synergistic regulation of elements in Group 15 (P, As, Sb) and Group 16 (S, Se, Te), as shown in Fig. 6f. Substitution of chalcogens at the α-position can red-shift the Q-band of free Pc to 809–835 nm; after introducing central high-valent metal ions of Group 15 (P(v), As(v), Sb(v)), the Q-band further extends to 1018–1056 nm. Among them, As(v) and Sb(v) complexes not only achieve a Q-band at 1018 and 1056 nm, respectively, but also exhibit near-infrared fluorescence from 960–1400 nm. Electrochemical analysis indicates that the central element significantly reduces the HOMO–LUMO energy gap ($\Delta E = 0.92$–1.10 eV), and molecular orbital calculations reveal that the orbital interaction between peripheral chalcogen atoms and the central element is the key mechanism. Notably, the photostability of P(v) Pc is superior to that of the commercial dye IR-1048.[91] The position of peripheral substituents significantly affects the magnitude of the red shift, with α-position substitution typically producing a stronger red-shifting effect compared to β-position substitution.[92] In summary, through the synergistic modification of central high-valence main-group metal ions (especially P(v)) and peripheral α-position strong electron-donating substituents (such as S and Se), the frontier orbital energy levels of Pc can be precisely tuned, significantly narrowing the HOMO–LUMO energy gap and achieving a directional red shift of the absorption spectrum towards the near-infrared region (>1000 nm). Recent studies have also revealed intriguing quantum phenomena in phthalocyanine-based systems. Wang *et al.* demonstrated molecular electronic chirality in CuPc molecules adsorbed on bilayer graphene, induced *via* twisted π–π stacking, with reversible switching of enantiomers achieved through STM tip manipulation at low temperatures.[93]

Pc compounds typically exhibit high chemical purity, tunable hydrophilic-lipophilic balance, good biocompatibility, and specific photophysical properties, such as strong near-infrared absorption, high molar extinction coefficient, and photostability, making them highly valuable for application in photodynamic therapy (PDT). For photodynamic therapy applications, Kocaağa *et al.* recently synthesized Schiff base-decorated In(III) and Zn(II) phthalocyanines that exhibit high singlet oxygen quantum yields ($\Phi\Delta = 0.85$ for InPc) and excellent *in vitro* PDT efficacy against PC3 prostate cancer cells, with pronounced ROS generation and apoptotic effects upon light irradiation.[94] The effectiveness of PDT is highly dependent on the targeting and accumulation ability of photosensitizers at the tumor site. The PDT process mediated by Pc follows a clear molecular photophysical pathway: under laser irradiation, Pc molecules transition from the ground state S_0 to the singlet excited state S_1, and then undergo intersystem crossing (ISC) to convert to the long-lived triplet excited state (T_1). The T_1-state Pc transfers energy to ground-state oxygen (O_2), generating highly reactive singlet oxygen ($^1O_2$). Singlet oxygen causes oxidative damage to biological macromolecules (such as proteins, lipids, and nucleic acids), ultimately leading to tumor cell apoptosis or necrosis. To enhance the PDT efficacy of Pc, researchers have addressed issues such as aggregation quenching, insufficient targeting, and tumor microenvironment adaptation through molecular design and nanoengineering strategies. In terms of molecular modification, the conjugate of histone deacetylase inhibitor (HDACi) and Zn/InPc can precisely regulate subcellular localization (such as mitochondria or nucleus) through substitution sites (peripheral/non-peripheral), achieving a half-maximal inhibitory concentration (IC_{50}) of 16.8 μM for MCF-7 breast cancer cells, and confirming that the HDAC6 inhibition pathway can synergistically enhance the oxidative damage effect.[95] The tert-butylsulfonyl-substituted Zn/PtPc derivative ($ZnSO_2tBu/PtSO_2tBu$) exhibits significant photochemical differentiation: PtPc exhibits ultra-high singlet oxygen quantum yield ($\Phi\Delta = 0.87$–0.99) due to the heavy atom effect, while ZnPc can simultaneously generate singlet oxygen ($\Phi\Delta = 0.45$–0.48) and hydroxyl radicals and other reactive oxygen species (ROS), making it more suitable for hypoxic microenvironments.[96] In terms of delivery system optimization, the loading of ZnPc onto cationic hafnium-based metal organic layer (Hf_{12}–Ir MOL) effectively inhibits molecular aggregation, resulting in a 12-fold increase in singlet oxygen yield. Leveraging the protonation characteristics of the carrier, mitochondrial targeting is achieved, achieving a tumor inhibition rate of > 99% and a cure rate of 40–60% in colon cancer models.[97] After encapsulating sulfonyl Pc in Pluronic P123 polymer micelles, cell uptake efficiency is significantly enhanced, achieving complete tumor clearance without recurrence in organoid and mouse tumor transplantation models (observation period ≥ 5 months). Furthermore, temperature-sensitive poly(dopamine) nanoparticles (APZ NPs) co-loaded with ZnPc and hydrogen sulfide (H_2S) donors trigger H_2S release through photothermal effects, simultaneously alleviating tumor hypoxia (inhibiting

mitochondrial complex IV and enhancing the PDT efficiency of ZnPc) and downregulating the expression of heat shock protein (HSP90) (reducing the resistance of tumor cells to photothermal therapy (PTT)), thus realizing a synergistic PDT-PTT mechanism and exhibiting significant antitumor activity in solid tumor treatment (Fig. 7).[98] Based on the excellent and tunable optical properties of Pc compounds, precise chemical modification and multifunctional nanocarrier design have effectively overcome their limitations in traditional PDT applications (such as aggregation quenching, insufficient targeting, and poor adaptability to hypoxic environments), significantly enhancing the therapeutic efficacy of PDT and expanding its application from tumor treatment to antibacterial and environmental remediation fields. Future research will continue to focus on strategies such as targeting ligand functionalization and immune microenvironment regulation to further optimize the performance of Pc-based PDT formulations and accelerate their clinical translation process.

Research on 2D Pc material systems is relatively scarce, yet they also exhibit excellent optical properties. Specific research progress is as follows: CuPc thin films prepared on glass substrates *via* thermal evaporation exhibit characteristic absorption in the B band (near-ultraviolet region, 300–400 nm) and Q band (visible region, 600–700 nm). The Q band includes dual peaks at 620 and 696 nm, corresponding to the $\pi \rightarrow \pi^*$ transitions of the dimer and monomer, respectively. When the substrate temperature is increased to 200 °C, the main peak of the Q band red shifts to 630 nm, indicating that the increase in grain size affects the electronic oscillation of the Cu center (Fig. 8a). The energy gap (E_g) of the thin film ranges from 1.525 to 1.609 eV, consistent with the α-phase structural characteristics.[99] In 2D ZnPc materials, visible light absorption over a wide range of 569–1100 nm can be achieved through molecular structure regulation. The position of the Q band absorption peak can be red-shifted by 46–210 nm through naphthalene/anthracene group substitution or nitrogen doping strategies. Among them, the low-symmetry 2D ZnPc-4 material exhibits split Q-band characteristics, as shown in Fig. 8b and c. These materials have significant potential for applications in organic photovoltaics. For example, by stacking heterostructures (such as a 2D ZnPc-1/ZnPc-4 bilayer structure), the energy conversion efficiency of solar cells can be increased to 14.04%, providing a new organic material platform for breaking through the efficiency limits of silicon-based batteries.[100] 2D indium chlorine phthalocyanine (InPcCl) thin films with different thicknesses prepared using thermal evaporation technology exhibit amorphous structural characteristics and unique optical properties. They show high transmittance in the visible light range (around 491 and 951 nm) and dual optical energy gaps (1.37 and 2.84 eV), which do not change with film thickness, indicating that oxidation contamination was effectively avoided during material growth. Their refractive index exhibits anomalous dispersion characteristics related to π–π* electronic transitions in the visible light region, while in the normal dispersion region (wavelength > 1200 nm), it decays regularly with increasing wavelength. The nonlinear optical parameters of the thin film (such as the third-order nonlinear susceptibility on the order of 10^{-12} esu) and the optical limiting response increase with film thickness. The 95 nm thick film exhibits optimal optical limiting performance under laser excitation at 632.8 and

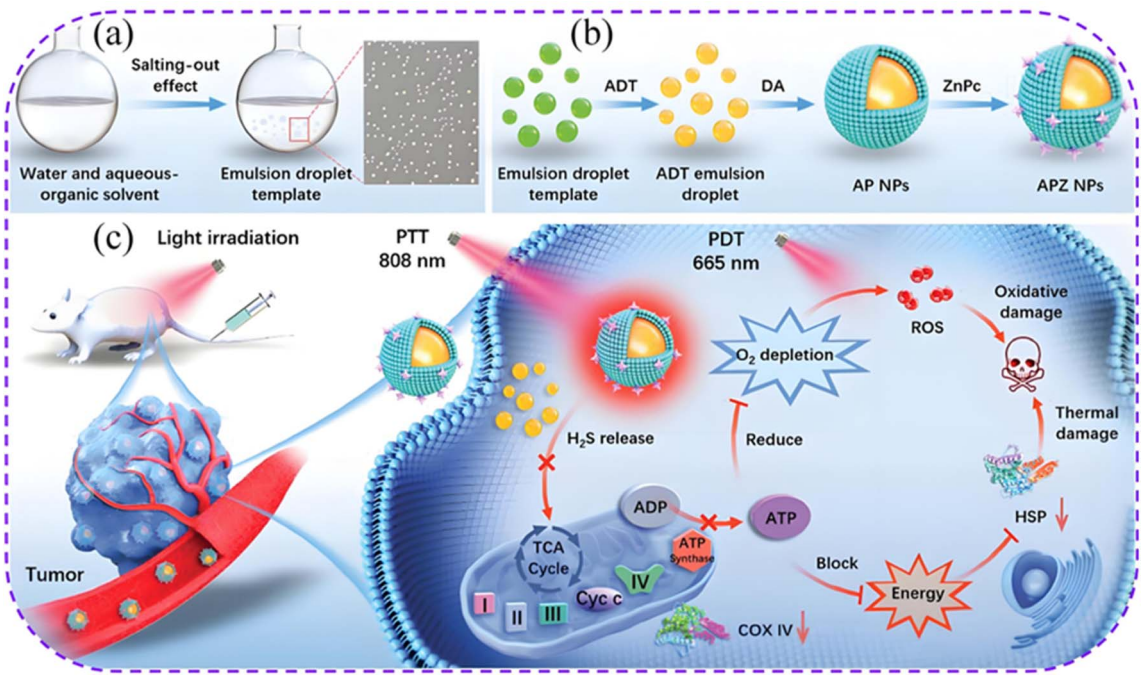

Fig. 7 The application of ZnPc in photodynamic therapy (PDT). Schematic diagram of (a) emulsion droplet template formation based on salting-out effect and (b) APZ NPs fabrication. (c) Schematic mechanism of APZ NPs in cancer treatment. Reproduced with permission from ref. 98. Copyright [2021] [American Chemical Society].

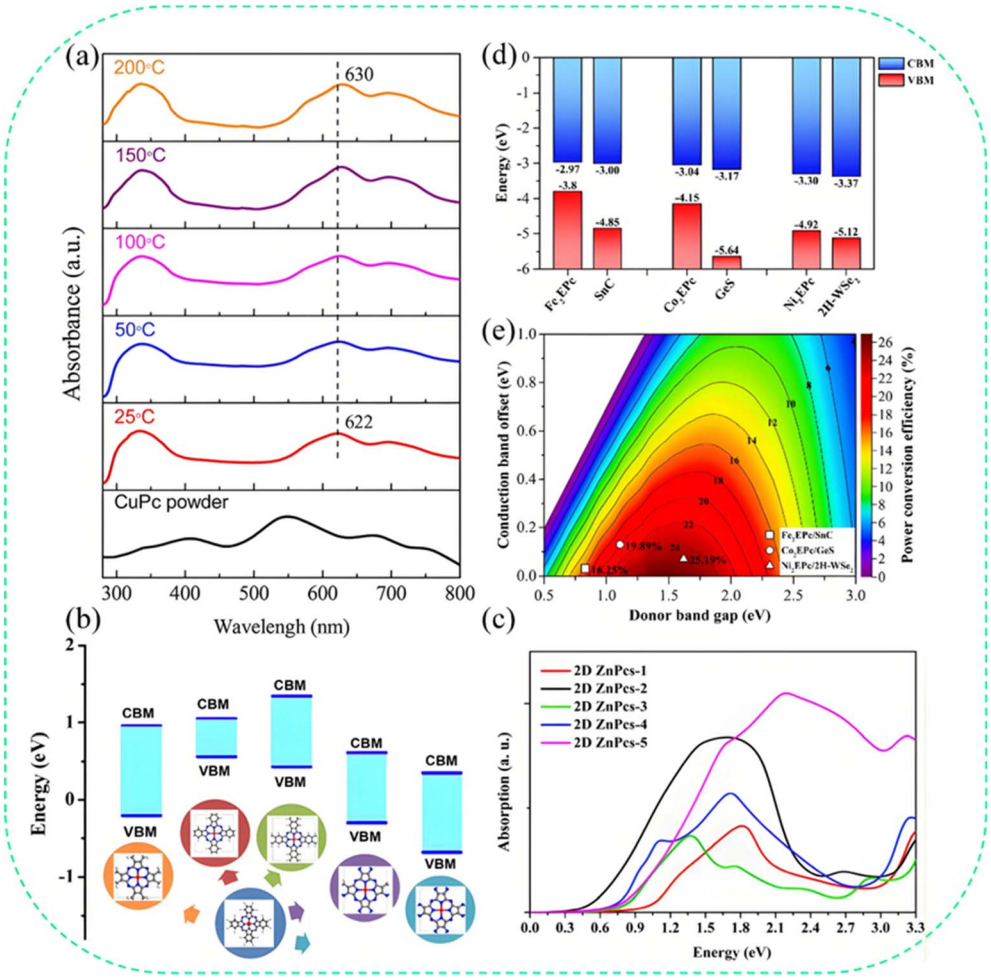

Fig. 8 Optical properties of 2D Pc materials. (a) The UV-vis spectra of CuPc powder and thin films prepared at different substrate temperatures. Reproduced with permission from ref. 99. Copyright [2018] [Elsevier, Ltd]. (b) The valence band maximum (VBM) and conduction band minimum (CBM) positions and (c) optical absorption spectra of a series of 2D ZnPc monolayers. Reproduced with permission from ref. 100. Copyright [2017] [AIP Publishing]. (d) Band alignment of VBM and CBM and (e) power conversion efficiencies (PCEs) of 2D type-II heterojunctions based on TM_2EPc monolayers. Reproduced with permission from ref. 103. Copyright [2024] [Wiley-VCH GmbH].

533 nm, demonstrating potential applications in photodetectors and optical limiting devices. Its performance can be further improved through film thickness tuning and synthesis process optimization.[101]

Furthermore, the study on constructing heterojunctions of the 2D material ReS_2 and zinc phthalocyanine fluoride (F_8ZnPc) indirectly reveals the crucial role of Pc materials in the photoelectronic process. F_8ZnPc exhibits ultrafast hole transfer characteristics (transfer time < 1 ns) with ReS_2, which, combined with the type II band alignment mechanism predicted by DFT calculations, verifies the potential application value of this system in polarization-sensitive photodetectors and long-lived photovoltaic devices, providing a new strategy for the performance optimization of organic/inorganic hybrid optoelectronic devices.[102] Additionally, the optical properties of 2D double transition metal extended phthalocyanine (TM_2EPc) materials can be significantly tuned through strain. For example, the light absorption intensity of Ni_2EPc increases by 79.4% under −8% compressive strain. Some systems (such as $Ni_2EPc/2H–WSe_2$ heterojunction) exhibit excellent photovoltaic properties, with energy conversion efficiency reaching 25.19%, which is superior to most excitonic solar cell materials (Fig. 8d and e). Strain can also induce an expansion of the light response range, such as the red shift of the absorption edge in V_2EPc under tensile strain, broadening the response in the visible light region. These changes in optical properties are closely related to the band structure and the hybridization strength of d-p orbitals, where the synergistic effect of N-2p and metal 3d orbitals dominates the photogenerated carrier separation efficiency, providing an important tuning dimension for the performance design of optoelectronic devices.[103]

3.2.3. Gap between theoretical predictions and experimental validation: challenges and perspectives. Despite the remarkable theoretical progress in predicting the electronic, magnetic, and optical properties of 2D phthalocyanine materials using density functional theory (DFT) and other computational methods, significant gaps remain between these predictions and experimental realizations. Addressing these

discrepancies is crucial for translating theoretical insights into practical applications.

3.2.3.1. Substrate effects on electronic structure. Most theoretical calculations assume freestanding 2D Pc monolayers in vacuum, neglecting the substantial influence of supporting substrates. Experimentally, 2D Pc materials are invariably synthesized or transferred onto substrates such as Au(111), Ag(111), SiO_2/Si, graphene, or h-BN, which can dramatically alter their electronic properties. For instance, theoretical predictions of the half-metallic ferromagnetic ground state in MnPc monolayers have been difficult to verify experimentally due to strong hybridization with metal substrates.[81] Abel *et al.* demonstrated that the electronic structure of FePc monolayers on Au(111) differs significantly from freestanding calculations, with substrate-induced charge transfer and orbital rehybridization altering the magnetic moment.[69] Similarly, the topological Dirac half-metal phase predicted in F-Pc COFs under 4% compressive strain has yet to be experimentally realized,[80] partly because achieving uniform strain in 2D Pc networks on rigid substrates remains challenging.

3.2.3.2. Material defects and disorder. Theoretical models typically assume perfect crystallinity with no defects, vacancies, or grain boundaries. However, experimentally synthesized 2D Pc materials invariably contain various defects. For example, liquid-phase exfoliated $Fe_{0.5}Co_{0.5}$Pc-CP nanosheets were found to be amorphous with complete loss of long-range crystallinity,[76] whereas theoretical predictions of high carrier mobility (19.4 $cm^2 V^{-1} s^{-1}$) were derived from perfectly crystalline polyarylene ether-based MPc frameworks.[77] The presence of sulfur vacancies in MoS_2-supported Pc hybrids has been shown to introduce mid-gap states that alter charge transfer dynamics.[84] Recent work by Li *et al.* demonstrated that the oxidation state and coordination environment of transition metal centers in Pc-based MOFs are highly sensitive to synthesis conditions, leading to significant variations in electrocatalytic activity that are not captured by idealized DFT models of perfect single-crystal structures.

3.2.3.3. Thermal stability and environmental degradation. The thermal stability and long-term environmental stability of 2D Pc materials represent another critical gap between theoretical predictions and experimental realities. While DFT calculations predict robust thermal stability for many 2D Pc networks, experimental studies have revealed that certain systems degrade under ambient conditions. For metal-free H_2Pc and many MPc systems, prolonged exposure to air, moisture, or light can lead to oxidation and decomposition. Theoretical predictions of strong binding energies for axial ligands (*e.g.*, 4.01 eV for F-FePc) and high thermal stability (>400 K) have not been systematically validated across the full range of 2D Pc materials.[86] Furthermore, the Curie temperature of MnPc predicted by Monte Carlo simulations (approximately 150 K) has not been experimentally confirmed,[81] as intrinsic ferromagnetism in 2D Pc monolayers remains challenging to isolate from substrate and defect contributions. In the context of catalytic applications, long-term operational stability (>100 hours) of 2D Pc electrocatalysts has rarely been demonstrated, despite theoretical predictions of high stability.[104,105]

3.2.3.4. Scaling laws and synthetic reproducibility. Another significant challenge is the scalability and reproducibility of 2D Pc materials. While surface synthesis under ultra-high vacuum produces atomically precise monolayers with exceptional quality,[69–71] the sample sizes are typically limited to tens to hundreds of nanometers, and the throughput is extremely low. Conversely, solution-based methods (solvothermal, microwave) offer scalability but produce nanosheets with wide distributions in thickness, lateral size, and crystallinity.[72–74,76] The mechanical exfoliation of Pc crystals yields larger flakes (several micrometers) but with low yield (<50%) and poor thickness control.[75] This scalability gap means that many theoretically predicted properties, such as high carrier mobility, topological states, and quantum anomalous Hall effects, have been verified only in a handful of ideal systems, and their translation to practical devices remains elusive.

3.2.3.5. Strategies to bridge the gap. To bridge the gap between theory and experiment, several strategies are being pursued. First, more sophisticated theoretical models that explicitly include substrate effects, defects, and finite-temperature dynamics are increasingly employed. For example, DFT + U calculations with Hubbard U parameters fitted to experimental X-ray absorption spectroscopy (XAS) data have improved the accuracy of electronic structure predictions for transition metal Pcs.[84] Second, *in situ* characterization techniques, such as *operando* XAS and Raman spectroscopy, are being developed to monitor structural and electronic changes under reaction conditions, enabling direct comparison with theoretical models. Third, machine learning approaches are being used to accelerate the exploration of the vast chemical space of 2D Pc materials and to predict properties that are more robust to defects and disorder. Finally, the development of scalable synthesis methods that yield high-quality, single-crystalline 2D Pc films on insulating substrates remains a critical priority for the field.

In summary, while theoretical calculations have provided invaluable guidance for the design of 2D Pc materials, the translation of these predictions into experimental realizations is often hindered by substrate effects, defects, thermal instability, and scalability challenges. Recognizing these gaps is essential for the rational design of next-generation 2D Pc materials with practical utility.

3.3. Applications of 2D phthalocyanine materials

After systematically elucidating the photophysical properties of 2D Pc materials (such as photoinduced electron transfer mechanisms and intramolecular charge transfer behavior), further attention is paid to their expanded applications as functionalized 2D platforms in the field of catalysis, gas detection and separation, and clean energy storage.

3.3.1. Catalytic applications. Empirical analysis based on DFT indicates that 2D Pc materials can efficiently drive key environmental catalytic reactions by regulating the coordination environment of metal active sites (such as single-atom Cr sites or Mn_2 dimer configurations). Among them, CrPc porous sheets achieve a low reaction energy barrier of 0.55 eV in low-

temperature CO oxidation and exhibit anti-poisoning characteristics, thanks to the selective orbital hybridization between Cr atomic d-orbitals and O_2/CO molecules;[104] while Mn_2Pc sheets utilize the synergistic bridge adsorption effect of bimetallic sites to significantly optimize the CO_2 electroreduction pathway ($CO_2 \rightarrow CH_3OH$), reducing the overpotential of the rate-determining step (*COOH formation) to 0.84 eV, breaking through the linear constraint of adsorption energy of traditional catalysts.[105] Further research shows that these materials also exhibit significant advantages in the electrocatalytic nitrogen reduction reaction (NRR): their stable Pc frameworks can anchor single/bimetallic active centers, achieving efficient adsorption and activation through the orbital interaction between metal d-orbitals and N_2 molecules (such as Ti_2-, V_2-, TiV-, VCr-, and VTa-Pc, as shown in Fig. 9a);[106] the introduction of boron doping to form non-metal-metal hybrid sites (such as B-modified expanded Pc) can construct a "push–pull" electron synergistic mechanism, significantly enhancing N≡N bond polarization (bond length extending to 1.54 Å) through the synergistic effect of B-sp^3 hybrid orbitals and metal d-orbitals, reducing the reaction limit potential to −0.24 V (such as FeNb-BPc), while the boron sites selectively capture H* to inhibit the hydrogen evolution side reaction, raising the Faraday efficiency to nearly 100%.[107] These achievements collectively reveal the universal strategy of 2D Pc materials in atomic-level active site design, reaction pathway optimization, and side reaction inhibition, providing a theoretical framework and material platform for the development of efficient heterogeneous catalytic systems. The molecular engineering of phthalocyanines for CO_2 electroreduction has been systematically reviewed by Santra *et al.*, who summarized recent advances in homogeneous and heterogeneous catalytic systems, including strategies such as hydrogen bonding, proton relay, bimetallic cooperative action, and flow-cell integration with gas diffusion electrodes.[108] Han and co-workers recently demonstrated molecularly engineered Co-phthalocyanine COFs with integrated boron and fluorine substituents for efficient nitric oxide-to-ammonia electroreduction, achieving an ammonia yield of 1166.67 μg cm^{-2} h^{-1} and a faradaic efficiency of 82.27%, the first experimental example of COFs for NORR.[109] Furthermore, Akiyama *et al.* developed an innovative strategy for enhancing ORR activity by supporting FePc on K^+-DB18C6-encapsulated single-walled carbon nanotubes. The electron doping of SWCNTs *via* molecular encapsulation modulates the electronic state of FePc, achieving an onset potential of 0.624 V *vs.* RHE and a nearly complete four-electron ORR pathway (n = 3.97).[110]

3.3.2. Gas detection and separation. In addition to the aforementioned catalytic performance, 2D Pc materials also exhibit multidimensional application value in the fields of gas detection, separation, and storage. Systematic studies based on DFT reveal that transition metal (such as Pd, Ru, Fe, Cr, Mn)

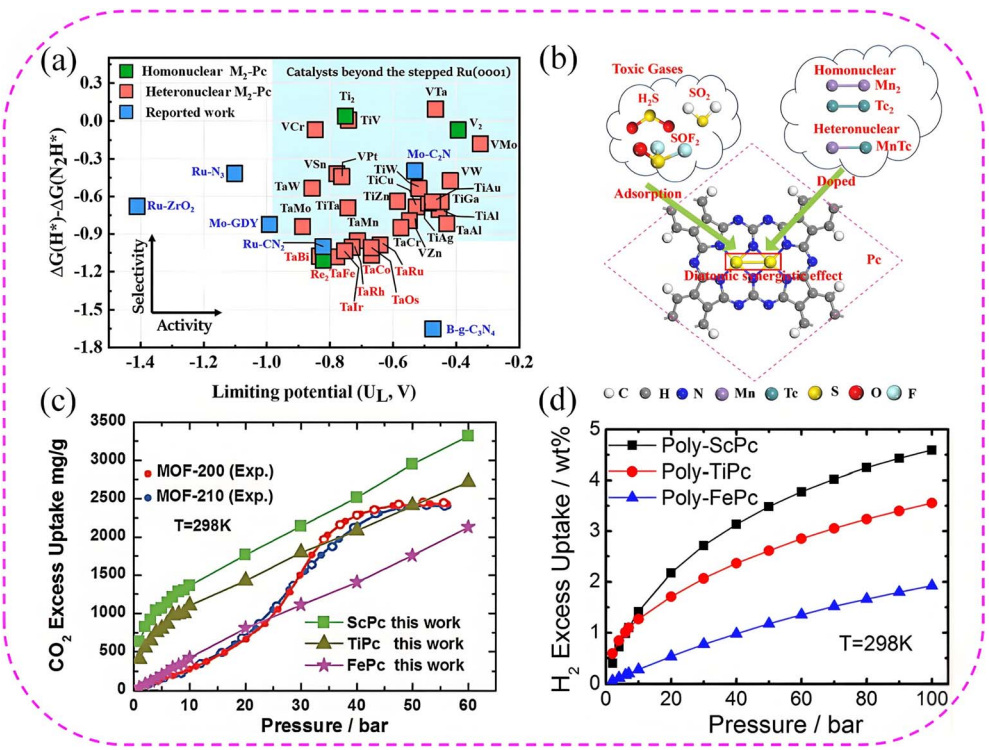

Fig. 9 (a) Limiting potential (U_L) *versus* $\Delta G(H^*)-\Delta G(N_2H^*)$ on 31 M_2-Pc catalysts. Reproduced with permission from ref. 106. Copyright [2024] [Springer Nature, Ltd]. (b) Schematic diagram of bimetallic phthalocyanine monolayer for detecting toxic gases H_2S, SO_2, and SOF_2. Reproduced with permission from ref. 112. Copyright [2024] [Springer Nature, Ltd]. (c) CO_2 excess adsorption isotherms for different TMPc (TM = Sc, Ti, Fe) sheets at T = 298 K. Reproduced with permission from ref. 115. Copyright [2024] [Springer Nature, Ltd]. (d) H_2 excess adsorption isotherms for TMPc (TM = Fe, Sc, Ti) at T = 298 K. Reproduced with permission from ref. 119. Copyright [2024] [Springer Nature, Ltd].

embedded 2D Pc monolayer materials achieve high-selectivity chemisorption (adsorption energy generally below −0.8 eV) through strong hybridization between the metal center's d orbitals and the p orbitals of target gas molecules (including formaldehyde, NH_3, NO_2, SO_2, CO, NO, and decomposition components of SF_6, as shown in Fig. 9b), while effectively suppressing background gas interference.[111,112] Such adsorption can significantly modulate the electronic properties of the material: inducing a semiconducting transition (bandgap increase of 0.4–1.2 eV), altering magnetic moment (such as a 72% decrease in magnetic moment after CrPc adsorbs NO),[113] and enhancing conductivity sensitivity (such as RuPc's sensitivity to formaldehyde reaching 1.65×10^7).[114] Their tunable desorption performance (such as MnPc's recovery time to SO_2 at room temperature is 0.91 ms) further supports the design of highly sensitive and reusable sensors.

In the field of gas separation, functionalized 2D Pc materials exhibit breakthrough performance. Transition metal-embedded Pc monolayers (such as ScPc) significantly enhance the adsorption capacity (2949 mg g^{-1} at 298 K and 50 bar) and selectivity for CO_2 through electrostatic interactions and electron transfer effects, providing a theoretical basis for high-sensitivity gas capture (Fig. 9c);[115] halogen-modified metal-free Pcs (such as F–H_2PPc) achieve efficient screening of mixed gases such as H_2/CO and CO_2/N_2 through precise control of sub-nanometer pore size, with permeability (10^{-3} mol m^{-2} s^{-1} Pa^{-1}) and selectivity (up to 10^{13}) improved by several orders of magnitude compared to traditional membrane materials.[116] Metal-modified systems (such as RuPc) respond rapidly to highly toxic phosgene ($COCl_2$) through chemical adsorption (−0.50 eV) and electron transfer (0.165 e), with bandgap changes (0 → 0.605 eV) that can be converted into electrical signals, and possess millisecond-level desorption capability (0.284 ms at 298 K).[117]

3.3.3. Clean energy storage. In the field of clean energy storage, 2D Pc materials also exhibit outstanding performance. Li-doped Pc covalent organic framework (Li-Pc-PBBA COF) utilizes stable bonding between Li ions and framework oxygen (binding energy of 1.08 eV) to adsorb hydrogen molecules through a charge polarization mechanism (average adsorption energy of 0.11 eV/H_2), achieving a theoretical hydrogen storage capacity of 5.3 wt%. The B substitution strategy further addresses the issue of Li agglomeration, increasing the binding energy to 2.06 eV and enhancing H_2 adsorption to 0.17 eV.[118] The ScPc monolayer utilizes Kubas interactions (H_2 → Sc charge donation and back-donation) at out-of-plane exposed Sc sites (protrusion height of 0.67 Å) to achieve an ideal adsorption energy (0.23 eV), achieving a hydrogen storage capacity of 4.6 wt% under near-operating conditions (298 K, 100 bar). The isolated metal site design effectively circumvents the agglomeration bottleneck (Fig. 9d).[119]

The aforementioned studies collectively unveil the synergistic application potential of 2D Pc materials in areas such as precise detection of toxic gases, efficient separation of mixed gases, and clean energy storage, achieved through strategies like metal active site design, halogen modification, and framework engineering. This provides a theoretical foundation for their multifunctional and integrated development.

4. Current challenges and future prospects

4.1. Current challenges

2D Pc materials, as a class of organic 2D materials with molecular designability and highly tunable electronic structures, exhibit unique potential in fields such as optoelectronic devices, energy conversion, and storage. However, their theoretical exploration and potential application development still face a series of key issues. The main challenges currently can be summarized as follows: (1) existing research is highly focused on transition metal Pcs (such as FePc, CoPc, CuPc, *etc.*), while research on Pc materials based on main-group elements (such as Al, Si, Sn, *etc.*) is relatively scarce. This to some extent limits the chemical diversity and structural designability of 2D Pc material systems, hindering the theoretical exploration and design of material systems with novel properties (such as superior optical bandgap and specific catalytic activity). (2) As revealed by the preliminary discussion on optical properties mentioned earlier, 2D Pc materials have potential optical application value. However, current research in the field is largely focused on the magnetic and spintronic properties of 2D Pcs and their regulation. There is a lack of systematic theoretical research on their core performance parameters in optoelectronics, such as photoresponse characteristics, photoelectric conversion mechanisms, and photovoltaic performance for solar energy conversion (such as energy conversion efficiency). (3) The vast majority of successfully constructed 2D Pc networks are limited to a single configuration (usually a tetragonal lattice formed by transition metal-nitrogen coordination, *i.e.*, MPc type). For other potential network structures (such as those based on different symmetries or connection sites), there is little research on their synthesis strategies, structural stability, and derivation of novel properties. The uniformity of configuration selection greatly limits the in-depth exploration of universal structure–property relationships in 2D Pc materials and also restricts the exploration and prediction of their potential functional diversity. (4) For optoelectronic device (especially photovoltaic device) applications, the E_g of 2D Pc semiconductors deviates from the optimal working range (1.1–1.7 eV). How to effectively optimize their bandgap and light absorption properties through reasonable chemical modification (such as central metal regulation, axial ligand modification) or physical means (strain engineering), and thereby optimize the theoretical prediction of their energy conversion efficiency to meet the basic requirements of future optoelectronic device applications, is one of the core challenges in current theoretical research.

4.2. Future prospects

To address the aforementioned issues and challenges in 2D Pc materials, this study intends to adopt the following core research strategies: (1) expanding the main-group element

system and discovering novel properties: in response to the issue of predominantly transition metal-based compositions, a series of 2D Pc materials based on main-group elements (such as Al, Si, Sn, *etc.*) will be designed. Through systematic research on their electronic structure, carrier mobility, and optical properties, the aim is to enrich the material system and discover unique physicochemical properties (such as unique Dirac electron states, more optimal bandgaps, or specific functionalities) that differ from those of transition metal Pcs. (2) Innovating 2D Pc network configurations and exploring structure–property relationships: Addressing the issue of a single network configuration, it needs to break through the limitations of the traditional tetragonal lattice (MPc type) to construct novel 2D Pc networks with diagonal connections and design dual-center metal-expanded Pcs. The goal is to explore, through computational simulations, the impact of different network structures on their electronic band structures, optical absorption characteristics, and carrier transport behavior, deepening the understanding of the "structure–property" relationship and providing new ideas for material functional design. (3) Utilizing chemical modification and physical regulation methods to achieve synergistic performance control: to address the core challenges of bandgap deviation from the optimal range and insufficient light absorption performance, it is necessary to systematically employ central metal substitution, axial ligand modification, and strain engineering to investigate their effects on the E_g, light absorption coefficient, and energy conversion efficiency of the materials. This will provide a basis for the theoretical design of efficient optoelectronic conversion materials.

5. Conclusion

2D Pc materials are constructed using structurally tunable and property-excellent Pc molecules as basic building blocks. Through precise synthesis strategies and diverse assembly methods, a novel functional material system that combines intrinsic molecular characteristics with 2D confinement effects has been developed. This article systematically reviews the molecular structural basis and synthesis methods of Pc compounds and deeply expounds on the construction strategies, electronic structure tuning, optical property evolution, and research progress in fields such as catalysis, gas sensing, and energy storage of 2D Pc materials. Research indicates that effective control over the material's band structure, magnetic ground state, light absorption range, and catalytic activity can be achieved through central metal substitution, peripheral substituent modification, axial coordination tuning, and strain engineering. Simultaneously, these materials exhibit promising potential in applications such as gas adsorption and separation, hydrogen storage, and electrocatalysis. Current research still faces challenges such as insufficient expansion of main-group element systems, limited network configurations, and weak research on optoelectronic properties. In the future, efforts should focus on enriching the material system, innovating network structures, and coordinating multi-dimensional tuning strategies to drive the development of 2D Pc materials towards high performance and multifunctionality. This review aims to provide a systematic theoretical reference for the rational design and application exploration of 2D Pc materials.

Conflicts of interest

The authors declare no competing financial interest.

Data availability

No primary research results, software or code have been included and no new data were generated or analysed as part of this review.

Acknowledgements

This work was supported by the National Natural Science Foundation of China (12504130), the Natural Science Foundation of Hubei Province (2024AFB364, 2024AFB424), and the Natural Science Foundation of Xiaogan Municipality (XGKJ2025010095).

References

1 C. Chang, W. Chen, Y. Chen, Y. Chen, F. Ding, C. Fan, *et al.*, Recent Progress on Two-Dimensional Materials, *Acta Phys. -Chim. Sin.*, 2021, **37**(12), 2108017.
2 J. Yang, Z. Chen, L. Zhang and Q. Zhang, Covalent Organic Frameworks for Photocatalytic Reduction of Carbon Dioxide: A Review, *ACS Nano*, 2024, **18**(33), 21804–21835.
3 S. Xu, J. Wu, X. Wang and Q. Zhang, Recent Advances in the Utilization of Covalent Organic Frameworks (COFs) as Electrode Materials for Supercapacitors, *Chem. Sci.*, 2023, **14**(47), 13601–13628.
4 J. Wu, S. Zhang, Q. Gu and Q. Zhang, Recent Progress in Covalent Organic Frameworks for Flexible Electronic Devices, *FlexMat*, 2024, **1**(2), 160–172.
5 J. Yang, F. Kang, X. Wang and Q. Zhang, Design Strategies for Improving the Crystallinity of Covalent Organic Frameworks and Conjugated Polymers: A Review, *Mater. Horiz.*, 2022, **9**(1), 121–146.
6 O. Abdulrahman Hamad, R. O. Kareem and P. Khdir Omer, Recent Developments in Synthesize, Properties, Characterization, and Application of Phthalocyanine and Metal Phthalocyanine, *J. Chem. Rev.*, 2024, **6**(1), 39–75.
7 R. P. Linstead, 212. Phthalocyanines. Part I. A New Type of Synthetic Colouring Matters, *J. Chem. Soc.*, 1934, 1016–1017.
8 J. M. Robertson, 136. An X-Ray Study of the Structure of the Phthalocyanines. Part I. The Metal-Free, Nickel, Copper, and Platinum Compounds, *J. Chem. Soc.*, 1935, 615–621.
9 O. Matsushita, V. M. Derkacheva, A. Muranaka, S. Shimizu, M. Uchiyama, E. A. Luk'yanets and N. Kobayashi, Rectangular-Shaped Expanded Phthalocyanines with Two Central Metal Atoms, *J. Am. Chem. Soc.*, 2012, **134**(7), 3411–3418.
10 H. Pekbelgin Karaoğlu and A. Kalkan Burat, A- and B-Substituted Metal-Free Phthalocyanines: Synthesis,

Photophysical and Electrochemical Properties, *Molecules*, 2020, **25**(2), 363.
11 K. Mitra and M. C. T. Hartman, Silicon Phthalocyanines: Synthesis and Resurgent Applications, *Org. Biomol. Chem.*, 2021, **19**(6), 1168–1190.
12 J. Mack and N. Kobayashi, Low Symmetry Phthalocyanines and Their Analogues, *Chem. Rev.*, 2011, **111**(2), 281–321.
13 C. G. Claessens, U. Hahn and T. Torres, Phthalocyanines: From Outstanding Electronic Properties to Emerging Applications, *Chem. Rec.*, 2008, **8**(2), 75–97.
14 C. Wang, N. V. Tkachenko, B. Song and L.-M. Yang, 2d P-Block Main Group Phthalocyanine Monolayers, *Adv. Energy Mater.*, 2025, **15**(33), 2502472.
15 Y. Li, M. S. Hassan, D. Chen, Y. Wu, X. Zhao, A. S. Portniagin, H. Liu, S. Wang, P. Ren, Y. Zhao and A. L. Rogach, Stacking Order-Mediated Spin-State Modulation in Iron Phthalocyanine Covalent Organic Frameworks Enables Efficient Oxygen Reduction Reaction, *ACS Appl. Mater. Interfaces*, 2026, **18**(4), 6735–6746.
16 X. Wang, S. Sun, J. Yao, H. Wan, R. Ma and W. Ma, Two-Dimensional Metallophthalocyanine Nanomaterials for Electrocatalytic Energy Conversion, *Energy Environ. Mater.*, 2024, **7**(4), e12709.
17 E. A. Mack, A. Cadranel, E. Harrer, X. Zhou, M. Wu, L. M. O. Lourenço, D. Zahn, E. Spiecker, C. Backes and D. M. Guldi, Morphological and Electronic Control of Interfacial Charge Transfer in 2d Transition Metal Dichalcogenide Hybrids, *ACS Nano*, 2025, **19**(31), 28576–28587.
18 D. Gounden, N. Nombona and W. E. van Zyl, Recent Advances in Phthalocyanines for Chemical Sensor, Non-Linear Optics (NLO) and Energy Storage Applications, *Coord. Chem. Rev.*, 2020, **420**, 213359.
19 N. Kobayashi, T. Furuyama and K. Satoh, Rationally Designed Phthalocyanines Having Their Main Absorption Band Beyond 1000 Nm, *J. Am. Chem. Soc.*, 2011, **133**(49), 19642–19645.
20 T. Alagöz, H. Genç Bilgiçli, E. Polat, H. Pişkin, B. Tüzün, A. Günsel, A. Erdoğmuş, M. N. Yaraşır and A. T. Bilgiçli, Ag(I) Induced H-Type and Pd(Ii) Induced J-Type Phthalocyanines to Enhance Pdt Applications: Synthesis, Optical Behaviors, Photochemical/Photophysical Properties, and Dft Studies, *Dalton Trans.*, 2025, **54**(25), 10052–10070.
21 N. Naeem, A. Sadiq, H. A. Ogaly and E. U. Mughal, Phthalocyanine-Nanoparticle Conjugates for Enhanced Cancer Photodynamic Therapy, *RSC Adv.*, 2025, **15**(36), 29890–29924.
22 W.-Z. Wang, H. Xu, Z. Chen, S. Fu, C. Wang and X. Li, Modulation of Phthalocyanine Assembly Morphology for Photodynamic Therapy, *Chem. Commun.*, 2025, **61**(99), 19596–19607.
23 Y. Choi, Y. Park, J. M. Kim, T. Kwon, S. Koo and D. W. Kang, Phthalocyanine-Based Metal-/Covalent Organic Frameworks and Their Photo/Electrochemical Applications, *Inorg. Chem. Commun.*, 2025, **182**, 115607.
24 M. Zambrano-Angulo and G. Cárdenas-Jirón, Charge Transport of Silicon(IV) and Zinc(II) Phthalocyanines by Molecular Junction Models, *J. Mater. Chem. C*, 2025, **13**(7), 3452–3464.
25 O. A. Hamad, R. O. Kareem and P. K. Omer, Recent developments in synthesize, properties, characterization, and application of phthalocyanine and metal phthalocyanine, *J. Chem. Rev.*, 2024, **6**(1), 39–75.
26 H. D. Diesbach and E. V. D. Weid, Quelques sels complexes des o-dinitriles avec le cuivre et la pyridine, *Helv. Chim. Acta*, 1927, **10**(1), 886–888.
27 R. P. Linstead, 212. Phthalocyanines. Part I. A new type of synthetic colouring matters, *J. Chem. Soc.*, 1934, 1016–1017.
28 J. M. Robertson, 136. An X-ray study of the structure of the phthalocyanines. Part I. The metal-free, nickel, copper, and platinum compounds, *J. Chem. Soc.*, 1935, 615–621.
29 O. Matsushita, V. M. Derkacheva, A. Muranaka, S. Shimizu, M. Uchiyama, E. A. Luk'yanets and N. Kobayashi, Rectangular-shaped expanded phthalocyanines with two central metal atoms, *J. Am. Chem. Soc.*, 2012, **134**(7), 3411–3418.
30 H. P. Karaoglu and A. K. Burat, α- and β-substituted metal-free phthalocyanines: Synthesis, photophysical and electrochemical properties, *Molecules*, 2020, **25**(2), 363.
31 K. Mitra and M. C. T. Hartman, Silicon phthalocyanines: Synthesis and resurgent applications, *Org. Biomol. Chem.*, 2021, **19**(6), 1168–1190.
32 B. Han, B. Liang, E. Zhang, J. Li, Y. Li, Q. Zhang, Z. Xie, H. Wang and J. Jiang, Phthalocyanine covalent organic frameworks: Dimensionality effect on third-order nonlinear optical properties, *Adv. Funct. Mater.*, 2024, **34**(42), 202404289.
33 H. Zhang, L. Li, J. Chen, J. Wang, Y. Liu, H. Zhang, Q. Wang, S. Wang and G. Yang, Phthalocyanine covalent frameworks doped in PMMA matrix as high performance nonlinear optical limiter, *Dyes Pigm.*, 2023, **219**, 111553.
34 A. K. May, J. Mack and T. Nyokong, Effect of pyrrole substitution on the optical limiting properties of 3,5-distyrylBODIPYdyes, *J. Porphyrins Phthalocyanines*, 2023, **27**(1), 591–599.
35 W. Ji, T. X. Wang, X. Ding, S. Lei and B. H. Han, Porphyrin- and phthalocyanine-based porous organic polymers: From synthesis to application, *Coord. Chem. Rev.*, 2021, **439**, 213875.
36 M. Yahya, Y. Nural and Z. Seferoglu, Recent advances in the nonlinear optical (NLO) properties of phthalocyanines: A review, *Dyes and Pigm.*, 2022, **198**, 109960.
37 Z. Şen, D. K. Tarakci, I. Gürol, V. Ahsen and M. Harbeck, Governing the sorption and sensing properties of titanium phthalocyanines by means of axial ligands, *Sens. Actuators, B*, 2016, **229**, 581–586.
38 Z. Cui, L. Wang, Y. Zhu, Y. Zhang and L. J. Wang, Solution-processed filamentous copper phthalocyanine films for enhanced NO_2 gas sensing at room temperature, *New J. Chem.*, 2024, **48**(3), 1254–1263.
39 A. K. Sharma, A. K. Debnath, D. K. Aswal and A. Mahajan, Room temperature ppb level detection of chlorine using

peripherally alkoxy substituted phthalocyanine/SWCNTs based chemiresistive sensors, *Sens. Actuators B*, 2022, **350**, 130870.

40 E. Venuti, R. G. D. Valle, I. Bilotti, A. Brillante, M. Cavallini, A. Calò and Y. H. Geerts, Absorption, photoluminescence, and polarized Raman spectra of a fourfold alkoxy-substituted phthalocyanine liquid crystal, *J. Phys. Chem. C*, 2011, **115**(24), 12150–12157.

41 T. Ghosh, Synthesis, thermotropic properties, and applications of porphyrin-based liquid crystals: A comprehensive review, *Curr. Org. Chem.*, 2024, **28**(11), 857–889.

42 K. K. Yadav, U. Narang, S. Bhattacharya and S. M. S. Chauhan, Copperii phthalocyanine as an efficient and reusable catalyst for the N-arylation of nitrogen containing heterocycles, *Tetrahedron Lett.*, 2017, **58**(31), 3044–3048.

43 L. Yao, J. Ding, X. Cai, L. Liu, N. Singh, C. C. L. Mccrory and B. Liu, Unlocking the potential for methanol synthesis *via* electrochemical CO_2 reduction using CoPc-based molecular catalysts, *ACS Nano*, 2024, **18**(33), 21623–21632.

44 H. Pan, Y. Ren, Q. Wang, J. Hu, Y. Zhang, K. Wang and J. Jiang, New vitality of covalent organic frameworks endued by phthalocyanine: Yesterday, today, and tomorrow, *Coord. Chem. Rev.*, 2025, **527**, 216404.

45 Ç. Oruç, A. Erkol and A. Altındal, Characterization of metal (Ag, Au)/phthalocyanine thin film/semiconductor structures by impedance spectroscopy technique, *Thin Solid Films*, 2017, **636**, 765–772.

46 J. Broadhurst, G. Mallia and N. Harrison, A prediction of high temperature magnetic coupling in transition metal phthalocyanines, *J. Chem. Phys.*, 2024, **161**(11), 114703.

47 M. Bazarnik, J. Brede, R. Decker and R. Wiesendanger, Tailoring molecular self-assembly of magnetic phthalocyanine molecules on Fe- and Co-intercalated graphene, *ACS Nano*, 2013, **7**(12), 11341–11349.

48 Z. T. Shen, L. M. She, Y. T. Yang, G. H. Cao, Y. Jia, P. Cui, S. Q. Shen and Z. Zhang, Tuning the quantum spin states of Co-phthalocyanine on good, semi-, and half-metals, *Phys. Rev. B*, 2024, **110**(17), 174407.

49 C. Lu, Z. Yu and J. Cao, Advancement in porphyrin/phthalocyanine compounds-based perovskite solar cells, *Chin. J. Struct. Chem.*, 2024, **43**(3), 100240.

50 T. Wang, W. Zhang, T. Li, Q. Xia, S. Yang, J. Weng, K. Chen, W. Chen, M. Liu, S. Du, X. Zhang and Y. Song, Electrochromic smart window based on transition-metal phthalocyanine derivatives, *Inorg. Chem.*, 2024, **63**(6), 3181–3190.

51 L. C. Nene and H. Abrahamse, Design consideration of phthalocyanines as sensitizers for enhanced sono-photodynamic combinatorial therapy of cancer, *Acta Pharm. Sin. B*, 2024, **14**(3), 1077–1097.

52 G. Y. Atmaca, K. Celep and A. Erdogmus, Application of comparative sonochemical, photochemical, and sono-photochemical methods to obtain new silicon phthalocyanine with high singlet oxygen efficiency, *J. Organomet. Chem.*, 2024, **1004**, 122952.

53 R. P. Linstead and A. R. Lowe, 214. Phthalocyanines. Part III. Preliminary experiments on the preparation of phthalocyanines from phthalonitrile, *J. Chem. Soc.*, 1934, 1022–1027.

54 H. Uchida, H. Tanaka, H. Yoshiyama, P. Y. Reddy, S. Nakamura and T. Toru, Novel synthesis of phthalocyanines from phthalonitriles under mild conditions, *Synlett*, 2002, **10**, 1649–1652.

55 H. Uchida, H. Yoshiyama, P. Y. Reddy, S. Nakamura and T. Toru, The synthesis of metal-free phthalocyanines from phthalonitriles with hexamethyldisilazane, *Bull. Chem. Soc. Jpn.*, 2004, **77**(7), 1401–1404.

56 A. Bilgin, B. Ertem and Y. Gök, Synthesis and characterization of novel metal-free phthalocyanines containing four cylindrical or spherical macrotricyclic moieties, *Tetrahedron Lett.*, 2003, **44**(36), 6937–6941.

57 J. Alzeer, P. J. C. Roth and N. W. Luedtke, An efficient two-step synthesis of metal-free phthalocyanines using a Zn(II) template, *Chem. Commun.*, 2009, **15**, 1970–1971.

58 C. J. Walsh and B. K. Mandal, A novel method for the peripheral modification of phthalocyanines. Synthesis and third-order nonlinear optical absorption of β-tetrakis (2,3,4,5,6-pentaphenylbenzene) phthalocyanine, *Chem. Mater.*, 2000, **12**(2), 287–289.

59 T. Ceyhan and Ö. Bekaroğlu, The synthesis of new phthalocyanines substituted with 12-membered diazadioxa macrocycles, *Monatsh. Chem.*, 2002, **133**(1), 71–78.

60 J. Li, S. Wang, S. Li, Q. Wang, Y. Qian, X. Li, M. Liu, Y. Li and G. Yang, One-pot synthesis and self-assembly of copper phthalocyanine nanobelts through a water-chemical route, *Inorg. Chem.*, 2008, **47**(4), 1255–1257.

61 B. Liu and H. C. Zeng, Hydrothermal synthesis of ZnO nanorods in the diameter regime of 50 nm, *J. Am. Chem. Soc.*, 2003, **125**(15), 4430–4431.

62 Z. Kang, E. Wang, B. Mao, Z. Su, L. Gao, S. Lian and L. Xu, Controllable fabrication of carbon nanotube and nanobelt with a polyoxometalate-assisted mild hydrothermal process, *J. Am. Chem. Soc.*, 2005, **127**(18), 6534–6535.

63 W. Ouellette, M. H. Yu, C. J. O'connor, D. Hagrman and J. Zubieta, Hydrothermal chemistry of the copper–triazolate system: A microporous metal–organic framework constructed from magnetic $\{Cu_3(\mu_3\text{-oh})(\text{triazolate})_3\}^{2+}$ building blocks, and related materials, *Angew. Chem., Int. Ed.*, 2006, **45**(21), 3497–3500.

64 Y. Wang, H. Zhang, G. Zhang and Y. Guo, Mechanical and Electronic Properties of 2d-Phthalocyanines under External Strain, *RSC Adv.*, 2015, **5**(115), 94645–94649.

65 C. G. Claessens, U. Hahn and T. Torres, Phthalocyanines: From Outstanding Electronic Properties to Emerging Applications, *Chem. Rec.*, 2008, **8**(2), 75–97.

66 I. El Ouedghiri-Idrissi, M. Lougdali, Z. Makir, O. A. Niasse and Z. Sofiani, Photoluminescence of Organic Thin Film Copper Phthalocyanine Cupc for Led Application, *Mater. Today Proc.*, 2022, **66**, 76–79.

67 Y. Li, J. Tan, X. Zhao, L. Zhao and X. Chen, Two-Dimensional Phthalocyanine-Based Covalent Organic

Frameworks as High-Performance Electrocatalysts for Oxygen Reduction and Oxygen Evolution, *Mater. Today Commun.*, 2023, **37**, 107157.

68 M. Koudia and M. Abel, Step-by-step on-surface synthesis: From manganese phthalocyanines to their polymeric form, *Chem. Commun.*, 2014, **50**(62), 8565–8567.

69 M. Abel, S. Clair, O. Ourdjini, M. Mossoyan and L. Porte, Single layer of polymeric Fe-Phthalocyanine: An organometallic sheet on metal and thin insulating film, *J. Am. Chemi. Soc.*, 2011, **133**(5), 1203–1205.

70 D. M. Sedlovets, M. V. Shuvalov, Y. V. Vishnevskiy, V. T. Volkov, I. I. Khodos, O. V. Trofimov and V. I. Korepanov, Synthesis and structure of high-quality films of copper polyphthalocyanine–2D conductive polymer, *Mater. Res. Bull.*, 2013, **48**(10), 3955–3960.

71 M. Koudia and M. Abel, Step-by-step on-surface synthesis: from manganese phthalocyanines to their polymeric form, *Chem. Commun.*, 2014, **50**, 8565–8567.

72 J. D. Yi, D. H. Si, R. Xie, Q. Yin, M. D. Zhang, Q. Wu, G. L. Chai, Y. B. Huang and R. Cao, Conductive two-dimensional phthalocyanine-based metal–organic framework nanosheets for efficient electroreduction of CO_2, *Angew. Chem., Int. Ed.*, 2021, **60**(31), 17108–17114.

73 M. Lu, M. Zhang, C. G. Liu, J. Liu, L. J. Shang, M. Wang, J. N. Chang, S. L. Li and Y. Q. Lan, Stable dioxin-linked metallophthalocyanine covalent organic frameworks (COFs) as photo-coupled electrocatalysts for CO_2 reduction, *Angew. Chem., Int. Ed.*, 2021, **60**(9), 4864–4871.

74 X. Wang, S. Sun, J. Yao, H. Wan, R. Ma and W. Ma, Two-dimensional metallophthalocyanine nanomaterials for electrocatalytic energy conversion, *Energy Environ. Mater.*, 2024, **7**(4), e12709.

75 M. Wang, H. Shi, P. Zhang, Z. Liao, M. Wang, H. Zhong, F. Schwotzer, A. S. Nia, E. Zschech, S. Zhou, S. Kaskel, R. Dong and X. Feng, Phthalocyanine-based 2D conjugated metal-organic framework nanosheets for high-performance micro-supercapacitors, *Adv. Funct. Mater.*, 2020, **30**(30), 2002664.

76 W. Liu, C. Wang, L. Zhang, H. Pan, W. Liu, J. Chen, D. Yang, Y. Xiang, K. Wang, J. Jiang and X. Yao, Exfoliation of amorphous phthalocyanine conjugated polymers into ultrathin nanosheets for highly efficient oxygen reduction, *J. Mater. Chem. A*, 2019, **7**(7), 3112–3119.

77 C. Yang, K. Jiang, Q. Zheng, X. Li, H. Mao, W. Zhong, C. Chen, B. Sun, H. Zheng, X. Zhuang, J. A. Reimer, Y. Liu and J. Zhang, Chemically stable polyarylether-based metallophthalocyanine frameworks with high carrier mobilities for capacitive energy storage, *J. Am. Chem. Soc.*, 2021, **143**(42), 17701–17707.

78 Y. Qiang, H. Cao, Y. Pan, Y. Chi, L. Zhao, Y. Yang, H. B. Li, Y. Gao, L. Sun and Z. Yu, Copper naphthalocyanine-based hole-transport material for high-performance and thermally stable perovskite solar cells, *Sci. China Chem.*, 2024, **67**(8), 2701–2709.

79 Y. Wang, H. Zhang, G. Zhang and Y. Guo, Mechanical and electronic properties of 2D-phthalocyanines under external strain, *RSC Adv.*, 2015, **5**(115), 94645–94649.

80 X. Ni, H. Huang and J. L. Brédas, Emergence of a two-dimensional topological dirac semimetal phase in a phthalocyanine-based covalent organic framework, *Chem. Mater.*, 2022, **34**(7), 3178–3184.

81 J. Zhou and Q. Sun, Magnetism of phthalocyanine-based organometallic single porous sheet, *J. Am. Chem. Soc.*, 2011, **133**(38), 15113–15119.

82 W. Jiang, S. Zhang, Z. Wang, F. Liu and T. Low, Topological band engineering of lieb lattice in phthalocyanine-based metal–organic frameworks, *Nano Lett.*, 2020, **20**(3), 1959–1966.

83 M. Mabrouk, R. Hayn and R. B. Chaabane, First-principle study of metal-organic frameworks of the 4d and 5d transition metal series with phthalocyanine and tetracyanobenzene, *Superlattices Microstruct.*, 2019, **130**, 122–126.

84 I. E. Brumboiu, S. Haldar, J. Lüder, O. Eriksson, H. C. Herper, B. Brena and B. Sanyal, Ligand effects on the linear response hubbard U: The case of transition metal phthalocyanines, *J. Phys. Chem. A*, 2019, **123**(14), 3214–3222.

85 J. Zhou and Q. Sun, Absorption induced modulation of magnetism in two-dimensional metal-phthalocyanine porous sheets, *J. Chem. Phys.*, 2013, **138**(20), 204706.

86 H. B. Wang, Y. Su and G. Chen, First-principles investigation of chemical modification on two-dimensional iron—phthalocyanine sheet, *Chin. Phys. B*, 2014, **23**(1), 018103.

87 D. Gounden, N. Nombona and W. E. van Zyl, Recent advances in phthalocyanines for chemical sensor, non-linear optics (NLO) and energy storage applications, *Coord. Chem. Rev.*, 2020, **420**, 213359.

88 J. Mack and N. Kobayashi, Low symmetry phthalocyanines and their analogues, *Chem. Rev.*, 2011, **111**(2), 281–321.

89 C. G. Claessens, U. Hahn and T. Torres, Phthalocyanines: From outstanding electronic properties to emerging applications, *Chem. Rec.*, 2008, **8**(2), 75–97.

90 N. Kobayashi, T. Furuyama and K. Satoh, Rationally designed phthalocyanines having their main absorption band beyond 1000 nm, *J. Am. Chem. Soc.*, 2011, **133**(49), 19642–19645.

91 T. Furuyama, K. Satoh, T. Kushiya and N. Kobayashi, Design, synthesis, and properties of phthalocyanine complexes with main-group elements showing main absorption and fluorescence beyond 1000 nm, *J. Am. Chem. Soc.*, 2014, **136**(2), 765–776.

92 T. Furuyama and N. Kobayashi, Azaporphyrin phosphorus(v) complexes: Synthesis, structure, and modification of optical properties, *Phys. Chem. Chem. Phys.*, 2017, **19**(24), 15596–15612.

93 H.-J. Qin, R.-J. Sun, J.-J. Liu, W.-A. Liao, D.-B. Wang, J. Yu, T.-H. Leng, C.-F. Liu, W.-H. Zhang and Y.-S. Fu, Molecular Electronic Chirality in Copper Phthalocyanine Induced *via* Twisted π-π Stacking on Bilayer Graphene, *Nat. Commun.*, 2026, **17**(1), 3130.

94 N. Kocaağa, A. Türkkol, C. Can Karanlık, M. D. Bilgin and A. Erdoğmuş, In Vitro Evaluation of Schiff Base-Decorated Phthalocyanines for Photodynamic Therapy in PC3

Prostate Cancer Cells, *Dalton Trans.*, 2026, **55**(15), 6024–6034.

95 A. Zhang, Q. Wei, Y. Zheng, M. Ma, T. Cao, Q. Zhan and P. Cao, Hydrogen sulfide delivery system based on salting-out effect for enhancing synergistic photothermal and photodynamic cancer therapies, *Adv. Healthc. Mater.*, 2024, **13**(27), 2400803.

96 B. Aru, A. Günay, G. Y. Demirel, A. G. Gürek and D. Atilla, Evaluation of histone deacetylase inhibitor substituted zinc and indium phthalocyanines for chemo- and photodynamic therapy, *RSC Adv.*, 2021, **11**(55), 34963–34978.

97 P. Repetowski, M. Warszyńska, A. Kostecka, B. Pucelik, A. Barzowska, A. Emami, Ü. İşci, F. Dumoulin and J. M. Dąbrowski, Synthesis, photo-characterizations, and pre-clinical studies on advanced cellular and animal models of Zinc(II) and Platinum(II) sulfonyl-substituted phthalocyanines for enhanced vascular-targeted photodynamic therapy, *ACS Appl. Mate. Interfaces*, 2024, **16**(37), 48937–48954.

98 G. T. Nash, T. Luo, G. Lan, K. Ni, M. Kaufmann and W. Lin, Nanoscale metal–organic layer isolates phthalocyanines for efficient mitochondria-targeted photodynamic therapy, *J. Am. Chem. Soc.*, 2021, **143**(5), 2194–2199.

99 X. Ai, J. Lin, Y. Chang, L. Zhou, X. Zhang and G. Qin, Phase modification of copper phthalocyanine semiconductor by converting powder to thin film, *Appl. Surf. Sci.*, 2018, **428**, 788–792.

100 X. Jiang, Z. Jiang and J. Zhao, Self-assembly 2D zinc-phthalocyanine heterojunction: An ideal platform for high efficiency solar cell, *Appl. Phys. Lett.*, 2017, **111**(25), 253904.

101 S. Alfadhli, H. A. M. Ali, E. F. M. El-Zaidia, R. A. S. Alatawi, A. A. A. Darwish and I. S. Yahia, Effect of thickness on structural and optical characteristics of indium phthalocyanine chloride thin films for photodiode devices, *J. Mater. Sci.: Mater. Electron.*, 2021, **32**(2), 1907–1917.

102 P. Valencia-Acuna, T. R. Kafle, P. Zereshki, H. Peelaers, W. L. Chan and H. Zhao, Ultrafast hole transfer from monolayer ReS_2 to thin-film F_8ZnPc, *Appl. Phys. Lett.*, 2021, **118**(15), 153104.

103 D. B. Long, N. V. Tkachenko, Q. Feng, X. Li, A. I. Boldyrev, J. Yang and L. M. Yang, Two-dimensional bimetal-embedded expanded phthalocyanine monolayers: A class of multifunctional materials with fascinating properties, *Adv. Funct. Mater.*, 2024, **34**(22), 2313171.

104 Y. Li and Q. Sun, The superior catalytic CO oxidation capacity of a Cr-phthalocyanine porous sheet, *Sci. Rep.*, 2014, **4**(1), 4098.

105 H. Shen, Y. Li and Q. Sun, CO_2 electroreduction performance of phthalocyanine sheet with Mn dimer: A theoretical study, *J. Phys. Chem. C*, 2017, **121**(7), 3963–3969.

106 X. Guo, J. Gu, S. Lin, S. Zhang, Z. Chen and S. Huang, Tackling the activity and selectivity challenges of electrocatalysts toward the nitrogen reduction reaction *via* atomically dispersed biatom catalysts, *J. Am. Chem. Soc.*, 2020, **142**(12), 5709–5721.

107 L. Jiao and L. Guo, Embedding double transition metal atoms in B-Modified two-dimensional carbon-rich conjugated frameworks for efficient ammonia synthesis, *Inorg. Chem.*, 2022, **61**(46), 18574–18589.

108 A. Santra, A. Ghatak, Z. Chen, J. Shen, J. Helsen, Y. Birdja, A. Aukauloo and C. Zhang, Molecular Engineering of Metalloporphyrins and Phthalocyanines for Homogeneous and Heterogeneous Co2 Electroreduction, *Chem. Sci.*, 2026, **17**(17), 8345–8371.

109 D. Han, Z. Wang, H. Duan, L. Yang, H. Zhang, E. Mariani, M. Gao, Z. Wei, X. Li, L. Han, Y. Shen, M. Xie, E. Cortés and D. Zhang, Molecularly Engineered Co-Phthalocyanine Covalent Organic Frameworks for Efficient Nitric Oxide-to-Ammonia Electroreduction, *J. Am. Chem. Soc.*, 2025, **147**(45), 41355–41366.

110 T. Akiyama, Y. Ishii and S. Kawasaki, Enhancement of Oxygen Reduction Activity of Iron Phthalocyanine Electrocatalyst Supported on Carbon Nanotubes through Molecular Encapsulation, *Phys. Chem. Chem. Phys.*, 2026, **28**(1), 721–729.

111 Z. Nie, C. Wang, R. Xue, G. Xie and H. Xiong, Two-dimensional FePc and MnPc monolayers as promising materials for SF_6 decomposition gases detection: Insights from DFT calculations, *Appl. Surf. Sci.*, 2023, **608**, 155119.

112 R. Xue, Y. Guo, H. He, Y. Zhang, N. Yang, G. Xie and Z. Nie, Bimetallic phthalocyanine monolayers as promising materials for toxic H_2S, SO_2, and SOF_2 gas detection: Insights from DFT calculations, *Langmuir*, 2025, **41**(6), 4059–4075.

113 Y. Ma, H. Xiong, L. Gan and G. Deng, Theoretical investigation of 2D FePc and CrPc monolayers as a promising gas sensor for detecting hazardous gases, *Mater. Today Commun.*, 2023, **35**, 106378.

114 R. Xue, C. Wang, Y. Wang, Q. Guo, E. Dai and Z. Nie, Metal embedded phthalocyanine monolayers as promising materials for toxic formaldehyde gas detection: Insights from DFT calculations, *Metals*, 2022, **12**(9), 1442.

115 K. Lü, J. Zhou, L. Zhou, X. S. Chen, S. H. Chan and Q. Sun, Pre-combustion CO_2 capture by transition metal ions embedded in phthalocyanine sheets, *J. Chem. Phys.*, 2012, **136**(23), 234703.

116 Z. Meng, Y. Zhang, Q. Shi, Y. Liu, A. Du and R. Lu, A remarkable two-dimensional membrane for multifunctional gas separation: Halogenated metal-free fused-ring polyphthalocyanine, *Phys. Chem. Chem. Phys.*, 2018, **20**(28), 18931–18937.

117 C. Wang, Y. Wang, Q. Guo, E. Dai and Z. Nie, Metal-decorated phthalocyanine monolayer as a potential gas sensing material for phosgene: A first-principles study, *ACS Omega*, 2022, **7**(25), 21994–22002.

118 J. H. Guo, H. Zhang, Z. P. Liu and X. L. Cheng, Multiscale study of hydrogen adsorption, diffusion, and desorption on Li-doped phthalocyanine covalent organic frameworks, *J. Phys. Chem. C*, 2012, **116**(30), 15908–15917.

119 K. Lü, J. Zhou, L. Zhou, Q. Wang, Q. Sun and P. Jena, Sc-phthalocyanine sheet: Promising material for hydrogen storage, *Appl. Phys. Lett.*, 2011, **99**(16), 163104.